

Recent changes in the precipitation-driving processes over the southern tropical Andes/ western Amazon

**Hans Segura, Jhan Carlo Espinoza,
Clementine Junquas, Thierry Lebel,
Mathias Vuille & Rene Garreaud**

Climate Dynamics

Observational, Theoretical and
Computational Research on the Climate
System

ISSN 0930-7575

Clim Dyn

DOI 10.1007/s00382-020-05132-6



Your article is protected by copyright and all rights are held exclusively by Springer-Verlag GmbH Germany, part of Springer Nature. This e-offprint is for personal use only and shall not be self-archived in electronic repositories. If you wish to self-archive your article, please use the accepted manuscript version for posting on your own website. You may further deposit the accepted manuscript version in any repository, provided it is only made publicly available 12 months after official publication or later and provided acknowledgement is given to the original source of publication and a link is inserted to the published article on Springer's website. The link must be accompanied by the following text: "The final publication is available at link.springer.com".



Recent changes in the precipitation-driving processes over the southern tropical Andes/western Amazon

Hans Segura¹ · Jhan Carlo Espinoza¹ · Clementine Junquas¹ · Thierry Lebel¹ · Mathias Vuille² · Rene Garreaud^{3,4}

Received: 9 August 2019 / Accepted: 13 January 2020

© Springer-Verlag GmbH Germany, part of Springer Nature 2020

Abstract

Analyzing December–February (DJF) precipitation in the southern tropical Andes—STA (12° S–20° S; > 3000 m.a.s.l) allows revisiting regional atmospheric circulation features accounting for its interannual variability over the past 35 years (1982–2018). In a region where in-situ rainfall stations are sparse, the CHIRPS precipitation product is used to identify the first mode of interannual DJF precipitation variability (PC1-Andes). A network of 98 rain-gauge stations further allows verifying that PC1-Andes properly represents the spatio-temporal rainfall distribution over the region; in particular a significant increase in DJF precipitation over the period of study is evident in both in-situ data and PC1-Andes. Using the ERA-Interim data set, we found that aside from the well-known relationship between precipitation and upper-level easterlies over the STA, PC1-Andes is also associated with upward motion over the western Amazon (WA), a link that has not been reported before. The ascent over the WA is a component of the meridional circulation between the tropical North Atlantic and western tropical South America—WTSA (80° W–60° W; 35° S–10° N). Indeed, the precipitation increase over the last 2 decades is concomitant with the strengthening of this meridional circulation. An intensified upward motion over the WA has moistened the mid-troposphere over WTSA, and as a consequence, a decreased atmospheric stability between the mid- and the upper troposphere is observed over this region, including the STA. We further show that, over the last 15 years or so, the year-to-year variability of STA precipitation (periodicity < 8 years) has been significantly associated with upward motion over the WA, while upper-level easterlies are no longer significantly correlated with precipitation. These observations suggests that the STA have experienced a transition from a dry to a wet state in association with a change in the dominant mode of atmospheric circulation. In the former dominant state, zonal advection of momentum and moisture from the central Amazon, associated with upper-level easterlies, is necessary to develop convection over the STA. Since the beginning of the 21st century, DJF precipitation over the STA seems to respond directly and primarily to upward motion over the WA. Beyond improving our understanding of the factors influencing STA precipitation nowadays, these results point to the need of exploring their possible implications for the long-term evolution of precipitation in a context of global warming.

Keywords Amazon-Andes connectivity · Altiplano precipitation · Amazon convection · South America atmospheric circulation

Electronic supplementary material The online version of this article (<https://doi.org/10.1007/s00382-020-05132-6>) contains supplementary material, which is available to authorized users.

✉ Hans Segura
hans.segura@univ-grenoble-alpes.fr

¹ Univ. Grenoble Alpes, IRD, CNRS, Grenoble INP, IGE, 38000 Grenoble, France

² Department of Atmospheric and Environmental Sciences, State University of New York at Albany, Albany, NY, USA

³ Center for Climate and Resilience Research (CR2, FONDAPE 15110009), Santiago, Chile

⁴ Department of Geophysics, Universidad de Chile, Santiago, Chile

1 Introduction

The tropics encompass the wettest regions of the world, receiving more than 50% of the global annual precipitation (Adler et al. 2003, 2018). Recent studies have documented changes in tropical precipitation variability since the 1990s, with an increase in extreme wet and dry events during the rainy and the dry season, respectively (Allan et al. 2010; Hsu et al. 2011; Kao et al. 2017; Adler et al. 2018; Gu and Adler 2018; Panthou et al. 2018). South America is home to the largest tropical rainforest of the world, the Amazon, and the highest mountain chain in the inner tropics, the Andes. A significant increase in precipitation and enhanced deep convection over the northern Amazon Basin, in the core of tropical South America, has been detected in the December–May (wet) season since the end of the 20th century, especially over its western and equatorial regions (Barichivich et al. 2018; Wang et al. 2018; Espinoza et al. 2019a, b). This increased convection over the northern Amazon Basin has been attributed to changes in the Walker cell over the tropical Pacific Ocean and the cell connecting tropical South America and the tropical Atlantic Ocean (Espinoza et al. 2016; Barichivich et al. 2018). The authors argued that the tropical North Atlantic warming has indeed intensified low-level easterlies, increasing moisture transport from the Atlantic Ocean towards the Amazon. This mechanism was also identified by Wang et al. (2018), who used the Community Atmosphere Model version 4 (CAM4) to show that the main factor responsible for the increased November–May precipitation over the Amazon, is the warming of the tropical North Atlantic.

In contrast to the equatorial Amazon, precipitation over the southern Amazon (southward of 15° S) has experienced a significant decline, especially in the September–November season (Marengo et al. 2011; Fu et al. 2013; Debortoli et al. 2015; Espinoza et al. 2016, 2019a). Espinoza et al. (2019a) also showed that the September–November rainfall decline over the 1982–2017 period is significantly associated with increased mid-tropospheric subsidence over the southern Amazon, but also with enhanced deep convection over the equatorial Amazon. Based on these results, the authors inferred that tropical North Atlantic warming impacts the Amazonian precipitation through a seasonal change in the meridional circulation between the tropical North Atlantic and tropical South America. According to these studies, it appears that changes in the atmospheric circulation in tropical South America, especially in the Amazon region, have occurred since the last decades of the 20th century and that they are mainly associated with the tropical North Atlantic warming.

Regarding precipitation in the southern tropical Andes (> 3000 m.a.s.l.; 20° S–12° S), the picture is much less

conclusive. For instance, Morales et al. (2012) showed that annual precipitation reconstructed from tree-ring growth in the western Altiplano during the period 1300–2006 CE displays a negative trend since the second half of the 20th century, while using in-situ precipitation data, the authors noticed that annual precipitation in the same region does not show significant trends. Possible trends are of special interest when it comes to austral summer precipitation, since it is an essential water resource for agriculture, ecosystem sustainability, and human consumption, especially in the Altiplano region (Garreaud et al. 2003; Vuille 2003a, b; Vizu and Cook 2007; Perry et al. 2014; Segura et al. 2019; Vera et al. 2019), where it is strongly associated with Amazonian convection. The main objective of this study is therefore to analyze long-term changes in December–February precipitation over the southern tropical Andes, including its mean values and interannual variability, and its relationship with the intensified convection observed over the western Amazon. To that end, we used the CHIRPS satellite precipitation product and in-situ precipitation data covering the upper-elevation zones of the Andes (> 3000 m.a.s.l.) between 20° S and 12° S. In addition, the ERA-interim reanalysis data set is used to evaluate temporal changes in the atmospheric circulation, connecting convection over the Amazon with precipitation over the southern tropical Andes.

This manuscript has the following structure. In Sect. 2, we give a brief review of prior studies related to December–February precipitation variability over the southern tropical Andes on different time scales. The December–February atmospheric circulation climatology over South America is also described in this section, since it constitutes important background information. We discuss the data sets and methods used in Sect. 3, and we present and describe our primary results in Sect. 4. This latter section is composed of three subsections. In the first one, we introduce the upward motion over the western Amazon as an explanatory mechanism for precipitation variability over the southern tropical Andes. The second and the third subsections are focused on how the increased convection over the western Amazon has influenced the long-term precipitation variability in the southern tropical Andes. A discussion of our results and the principal conclusion of this study are presented in Sect. 5.

2 Background

The southern tropical Andes are characterized by a particular geographical configuration, with the wet and warm Amazon region to the east and the dry and cold eastern tropical Pacific to the west. Therefore, the spatial pattern of precipitation over this Andean region is characterized by a strong east–west gradient (e.g. Bendix and Lauer 1992; Houston

and Hartley 2003; Garreaud 2009; Espinoza et al. 2015). The complex topography and the low density of stations make it difficult to accurately characterize the spatio-temporal precipitation variability in this region. Segura et al. (2019) showed that the upper-elevation southern tropical Andes (> 3000 m.a.s.l and south of 8° S) shares a similar seasonal and interannual precipitation variability. Confirming previous studies, the authors demonstrated that the annual cycle of precipitation in this region is unimodal with a peak in December–March representing 75% of the total annual precipitation (Garreaud et al. 2003; Vuille and Keimig 2004).

December–March precipitation over the southern tropical Andes is associated with the development of the so-called

Bolivian High (BH), an anticyclonic system between 400 and 200 hPa (Fig. 1a; Virji 1981; Lenters and Cook 1997; Vuille et al. 1998; Garreaud et al. 2003; Vuille and Keimig 2004; Garreaud 2009). The anticyclonic circulation around the BH produces upper-level easterlies over the southern tropical Andes, especially over the Altiplano. As a consequence, zonal winds at 200 hPa (U200) over the southern tropical Andes have often been used as an index for depicting the intensity and position of the BH. Furthermore, several studies have evidenced a strong and significant relationship between December–March precipitation and U200 over this region on different time scales: diurnal (Junquas et al. 2018), intraseasonal (Garreaud 2000; Sicart et al.

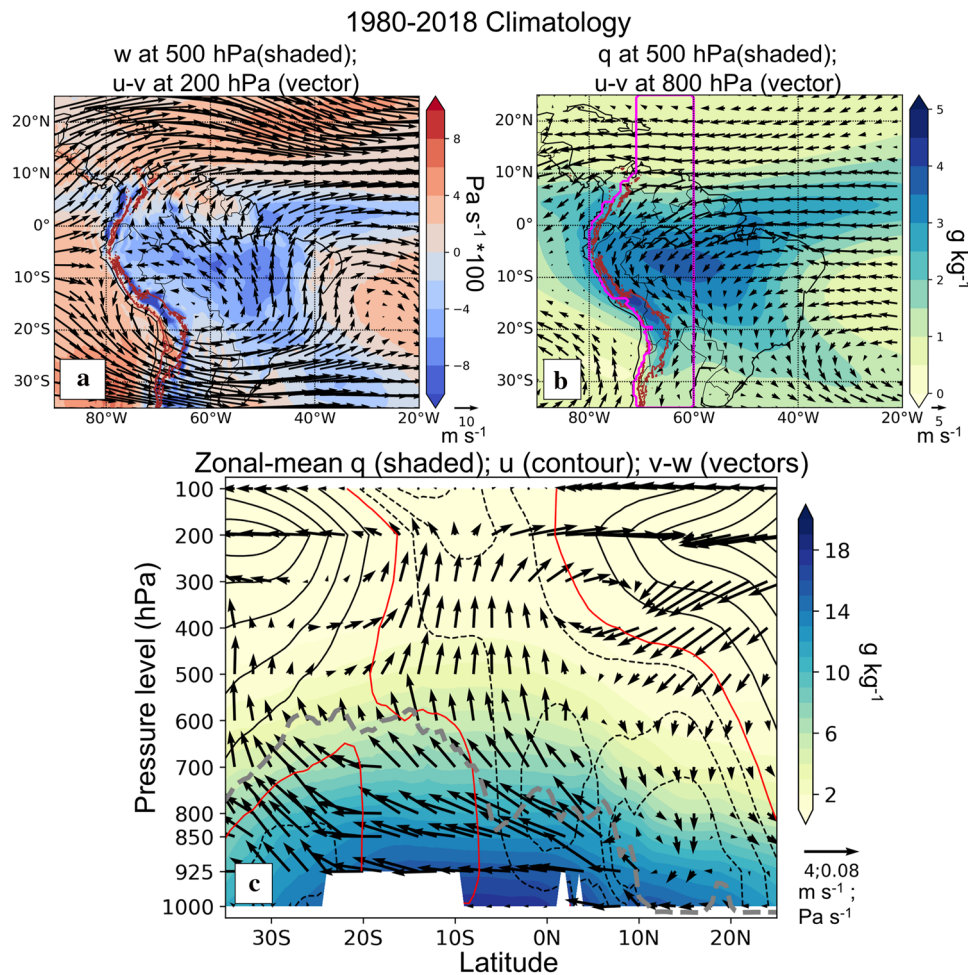


Fig. 1 **a** 1982–2018 climatology of vertical motion (w) at 500 hPa (shaded; Pa s^{-1}) and horizontal winds (u, v) at 200 hPa (vector; m s^{-1}). **b** 1982–2018 climatology of specific humidity (q) at 500 hPa (shaded; g kg^{-1}) and horizontal winds at 800 hPa (m s^{-1}). Values of w are multiplied by 100. In **a, b** the 3000 m.a.s.l. contour is shown as a crimson line. In **b** the magenta line highlights the region over which the zonal-mean is calculated. **c** Pressure-latitude cross section showing 1980–2018 climatology of December–February (DJF) zonal-mean meridional circulation (meridional- v and vertical- w winds; vectors), zonal winds (u ; contours) and specific humidity (q ; shaded)

in the tropical North Atlantic and western tropical South America. Westerlies (easterlies) are shown in solid (dashed) lines and the contour interval is 5 (2) m s^{-1} . Red line represents the 0 m s^{-1} of zonal wind contour. Zonal-mean is calculated using v, w, u and q in the region delimited by the magenta line in Fig. 1b. The dashed gray line represents the Andes' profile. The profile is calculated as the maximum topography elevation according to the ERA-Interim reanalysis data set. The atmospheric data are retrieved from the ERA-Interim reanalysis data set

2016), seasonal (Garreaud 1999; Segura et al. 2019), inter-annual (Vuille et al. 2000; Garreaud and Aceituno 2001; Minvielle and Garreaud 2011; Sulca et al. 2018; Segura et al. 2019; Vera et al. 2019) and decadal (Segura et al. 2016). The physical mechanism of this relationship relies on the introduction of easterly (westerly) momentum flux from the mid- and upper troposphere toward lowlands in the eastern Andes, which enhances (prevents) moisture-laden near-surface upslope flow (Garreaud 1999). In addition, Falvey and Garreaud (2005) highlighted the importance of the mid-tropospheric zonal moisture transport from the central Amazon in developing convection over the Altiplano. It is worth noting here that the role played by moisture transport in the mid-troposphere (700–400 hPa) in the development of deep convection in tropical regions, essentially by decreasing dry entrainment in clouds, was pointed in several studies (e.g. Zhang and Chou 1999; Sassi et al. 2001; Wu et al. 2009; Sherwood et al. 2010).

The interannual December–March precipitation variability in the southern tropical Andes is associated with sea surface temperature (SST) variability in the central Pacific (El Niño–La Niña events; e.g. Aceituno and Garreaud 1995; Vuille et al. 2000; Garreaud and Aceituno 2001; Vuille and Keimig 2004; Lagos et al. 2008; Vuille et al. 2008; Sulca et al. 2018). Warm (cold) SST anomalies in the central Pacific are associated with anomalous upper-level westerlies (easterlies) over the southern tropical Andes, which inhibit (enhance) convection and precipitation over this Andean region (Garreaud 1999). Furthermore, the influence of the central Pacific SST variability on December–March precipitation over the southern tropical Andes has also been highlighted on decadal time scales (Segura et al. 2016).

On the other hand, the Amazon Basin was shown to be the main moisture source for precipitation over the southern tropical Andes (Vuille 2003a, b; Martinez and Dominguez 2014; Perry et al. 2014). Indeed, the BH is a product of deep convection over the continental South Atlantic Convergence Zone, which includes the central Amazon and central and southeastern Brazil, during the mature phase of the South American Monsoon System or SAMS (Silva Dias et al. 1983; DeMaria 1985; Figueroa et al. 1995; Lenters and Cook 1997; Gandu and Silva Dias 1998; Rodwell and Hoskins 2001). The SAMS is related to a climatological intensification of low-level winds and moisture transport from the tropical Atlantic Ocean toward the southern tropical continent (Fig. 1b; e.g. Virji 1981; Vera et al. 2006; Nie et al. 2010). This process is associated with increased vertical moisture transport from lower to upper-tropospheric levels, which is a necessary condition for developing deep convection over the Amazon region (Fig. 1a,b; Zhou and Lau 1998; Schiro et al. 2016; Sakaguchi et al. 2018). Indeed, Nie et al. (2010) showed that the meridional circulation associated with the SAMS is characterized by a strong ascending branch south of the Equator (18° S–0° N)

and low-level northerlies originating over the Northern Hemisphere (see Figure 8c in Nie et al. 2010).

In order to capture how the meridional circulation and moisture transport between the tropical North Atlantic and western tropical South America might influence the relationship between convection over the western Amazon and precipitation over the southern tropical Andes, we computed the zonal-mean of meridional winds and vertical motion from the ERA-Interim reanalysis data set at different pressure levels (1000–100 hPa) inside the region delimited by the magenta line in Fig. 1b (Fig. 1c). This procedure was also done for zonal winds and specific humidity (Fig. 1c). The domain is configured so as to avoid being influenced by the particularities of the Caribbean region to the North, on the one hand, and by the radically different low-level atmospheric circulation over the eastern Pacific, on the other hand.

During the December–February season the ascending branch of the meridional circulation over western tropical South America is located over the western Amazon (15° S–0° N), and is connected to low-level northerlies and upper-level southerlies that cross the Equator (Fig. 1c). Low-level northerlies originate in the tropical North Atlantic (10° N–20° N) and cross northern South America (0° N–10° N) until reaching the western Amazon region (15° S–0° N). Meridional winds in the opposite direction are observed at upper-levels between the western Amazon region and the tropical North Atlantic. This implies that there is an exchange of energy and mass between the Southern and the Northern Hemisphere, in agreement with our current understanding of monsoon systems (Bordoni and Schneider 2008; Schneider and Bordoni 2008). Another characteristic of monsoon systems is the presence of upper-level easterlies over the ascending branch (dashed lines in Fig. 1c). This meridional circulation and the associated upper-level easterlies over its ascending branch have previously been diagnosed by Gill (1980) and Silva Dias et al. (1983) based on theoretical considerations. These mechanisms are in fact a response to the diabatic heating released over regions of deep tropical convection (in this case the South American monsoon). South of this meridional circulation cell a westerly regime prevails in the mid- and the upper troposphere (as expected from Bordoni and Schneider 2008; Schneider and Bordoni 2008; Nie et al. 2010). The transition between easterlies and westerlies is observed between 20° S and 15° S, as indicated by the red line in Fig. 1c. At 200 hPa, this red line signals the latitude at which the BH is centered as it is observed in Fig. 1a.

3 Materials and methods

3.1 Data

3.1.1 Satellite precipitation over the high Andes

We used The Climate Hazard group Infrared Precipitation with Stations (CHIRPS; Funk et al. 2015) data set to analyze the December–February precipitation variability over the region already defined in the introduction (20° S–12° S, above 3000 m.a.s.l.; Fig. 2a). This region, which largely intersects the Altiplano region, will be generically referred to in the following as the southern tropical Andes (note that in other publications, the area is rather named-Central Andes-, being in the middle of the Cordillera that extends from Patagonia to Colombia). The high spatial resolution (0.05° × 0.05°) and the temporal coverage from January 1981 to December 2018 make CHIRPS a suitable satellite precipitation product to study the precipitation variability over the complex topography of the Andes, as shown in previous studies (Paccini et al. 2018; Sulca et al. 2018; Segura

et al. 2019). The SRTM digital elevation product was interpolated to match the CHIRPS resolution, to allow selection of the grid points of the December–February precipitation field corresponding to our study domain.

3.1.2 In-situ records

In this study, we made use of 98 rain-gauge stations over the Altiplano: 79 from the National Service of Meteorology and Hydrology (SENAMHI) of Peru and 28 from the project “Data on climate and Extreme weather for the Central Andes” (DECADE; Hunziker et al. 2017). The in-situ precipitation data set covers the period from 1982 to 2015 at a monthly time step. More specific details regarding the rain-gauges are listed in Table S1. For any given year and station, December–February precipitation is computed only if all 3 monthly values of the December–February season are available; otherwise it is treated as a missing value. Based on that criterion, we found that the maximum number of years with missing data is three (3).

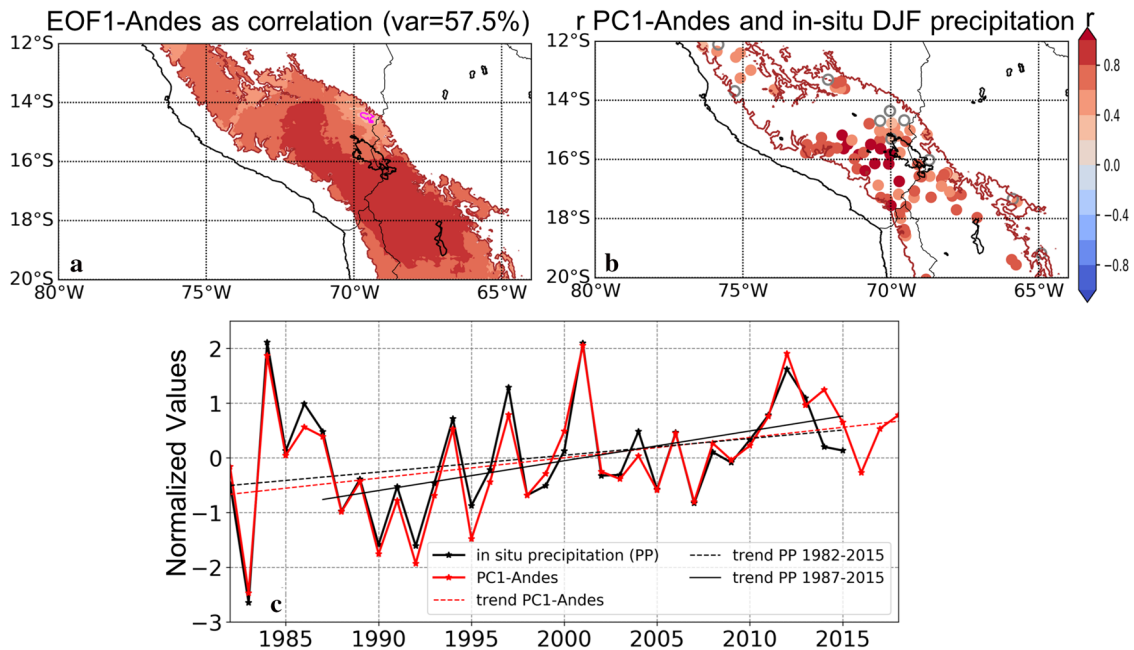


Fig. 2 **a** Spatial pattern of the first EOF mode of December–February (DJF) precipitation variability over the southern tropical Andes (PP-Andes; > 3000 m.a.s.l.; 12° S–20° S) for the 1982–2018 period shown as correlation coefficients between the first principal component of PP-Andes (PC1-Andes) and the original CHIRPS fields (shaded). The EOF analysis is carried out on the PP-Andes DJF fields for the 1982–2018 period. The 95% significance level is shown as a magenta line. **b** Correlation values between DJF in-situ precipitation (98 rain-gauge stations) and PC1-Andes for the 1982–2015 period. Colored (white) circles represent correlation values that are significant (non-signif-

icant) at the 95% confidence level. **c** PC1-Andes (red line) and the mean normalized in-situ precipitation in the southern tropical Andes (PP; black line). PP is calculated using the normalized DJF precipitation of 98 rain-gauge stations located in the southern tropical Andes, as shown in **b**. The 98 rain-gauge stations only cover the 1982–2015 period. The linear trend is shown for PC1-Andes (red dashed line, significant at p value < 0.05) using a Kendall-test. For PP, linear trends are estimated for the 1982–2015 period (dashed black line, p value < 0.1) and the 1987–2015 period (solid black line; p value < 0.01). In **a**, **b** the 3000 m.a.s.l. contour is shown as a crimson line

3.1.3 Atmospheric and sea surface temperature data sets

We used specific humidity, equivalent potential temperature, zonal and meridional wind and vertical motion at pressure levels between 1000 and 100 hPa from the ERA-Interim reanalysis (<http://apps.ecmwf.int/datasets/data/interim-full-daily/>; Dee et al. 2011). This reanalysis data set is available from January 1981 to December 2018 at a monthly time step and with a spatial resolution of $0.5^\circ \times 0.5^\circ$. Next, for each variable the interannual variability of the December–February season is analyzed.

3.2 Methods

3.2.1 Empirical orthogonal function

The empirical orthogonal function (EOF) method was used to obtain the leading mode of the spatio-temporal December–February precipitation variability over our domain of study. With the aim of avoiding that the EOF analysis might be biased by the strong west–east precipitation gradient across the southern tropical Andes, precipitation at each grid point was normalized using its historical mean and standard deviation before the EOF analysis was applied. The spatial pattern associated with the first mode of December–February precipitation over the southern tropical Andes is referred as EOF1-Andes while the principal component is denoted as PC1-Andes. EOF1-Andes is presented as the correlation field between precipitation at each grid point and PC1-Andes.

3.2.2 Butterworth filter

Segura et al. (2016) showed that austral summer precipitation over the southern tropical Andes presents a significant decadal and interdecadal variability (periods > 8 years). With the objective of analyzing changes in the interannual variability of December–February precipitation over the southern tropical Andes, we applied a Butterworth high-pass filter to the first principal component PC1-Andes. The Butterworth filter uses a cutoff frequency to keep only the frequencies of interest when analyzing the power spectrum of a time series. The power spectrum values of the relevant frequencies are multiplied by one (1), while those of the frequencies to be discarded, are multiplied by zero (0). An interesting feature of the Butterworth filter is that it allows controlling the sharpness applied to the frequency cutoff. This is referred to as the order of the filter. A small (large) order value means a soft (sharp) transition between relevant and discarded frequencies (Roberts and Roberts 1978). The Butterworth filter has been widely used to analyze precipitation and other meteorological variables in different regions (e.g. Zeng et al. 2008; Gouirand et al. 2012; Berntell et al.

2018) including the Altiplano (Melice and Roucou 1998; Segura et al. 2016). In this study, the interannual (decadal) variability is composed of all frequencies higher (lower) than 0.125 year^{-1} or periods lower (higher) than 8 years. The computation of the interannual variability of PC1-Andes was done as follows. First, we used the Butterworth filter with an order of 5 to obtain the decadal variability of PC1-Andes. Then, we subtracted this decadal time series from the original PC1-Andes to obtain the interannual variability of PC1-Andes. The same procedure was applied to all atmospheric variables discussed later.

3.2.3 Trend analysis

We used the Kendall test with a significance level at 95% to evaluate precipitation trends. The slope of the trend is calculated using a linear regression. For the CHIRPS data set we analyzed the 1982–2018 period, while in-situ precipitation trends were computed for the 1982–2015 period. A trend analysis was also applied to atmospheric variables for the period 1980–2018.

4 Results

4.1 Atmospheric mechanisms associated with the interannual variability of December–February precipitation

Figure 2a shows, based on correlation coefficients, the spatial pattern of the first mode of precipitation variability in the southern tropical Andes (EOF1-Andes), while the associated principal component (PC1-Andes) is displayed in Fig. 2c. The high percentage of explained variance by EOF1-Andes (57.5%) and the high correlation coefficients over most of the southern tropical Andes indicate that the interannual variability of December–February precipitation is likely controlled by the same mechanisms over the entire region, consistently with the results of Segura et al. (2019). The high and significant correlation coefficients between PC1-Andes and in-situ precipitation (Fig. 2b) show that PC1-Andes, while computed using CHIRPS, adequately represents the regional interannual precipitation variability within our zone of study. As a logical consequence, the mean normalized in-situ precipitation (black line in Fig. 2c), calculated using normalized December–February precipitation from each rain-gauge station, is significantly related to PC1-Andes for the 1982–2015 period ($r = 0.94$; $p \text{ value} < 0.05$). Notably, PC1-Andes shows a linear increase over the 1982–2018 period, indicating a positive trend in December–February precipitation in the southern tropical Andes. The significance of this precipitation increase and its associated atmospheric circulation will be covered in Sect. 4.2.

Several studies have evidenced the strong relationship between December–February precipitation and zonal winds at 200 hPa (U200) over the southern tropical Andes (see Sect. 2). This is confirmed by Fig. 3a, which displays a negative and significant (p value < 0.05) correlation between PC1-Andes and U200 over the region between 20° S– 10° S and 80° W– 60° W. Furthermore, a correlation analysis between PC1-Andes and vertical motion at 500 hPa (Pa s^{-1}) shows that an intensified upward motion over the western Amazon (80° W– 60° W), especially between 10° S and 0° N, is significantly associated with increases in precipitation over the southern tropical Andes (Fig. 3b). It is worth pointing out here that the link between the upward motion and the low-level meridional flow, both being components of the meridional circulation in western tropical South America, has been shown in Fig. 1c.

A correlation analysis for the 1982–2018 period between PC1-Andes and the interannual variability of zonal winds and specific humidity over western tropical South America and the tropical North Atlantic Ocean at different tropospheric levels shows two important features (Fig. 4) specifically localized between 25° S and 15° S, the region where the Altiplano is located: (1) a significant negative correlation between PC1-Andes and zonal winds above 600 hPa, and (2) a significant positive correlation between PC1-Andes and specific humidity in the mid-troposphere (600–400 hPa). These two characteristics have been analyzed in previous studies and, indeed, they are physically related (Garreaud 1999; Vuille and Keimig 2004).

Figure 4 also displays significant regression coefficients between PC1-Andes and vertical motion above 700 hPa between 10° S and 0° N, and with the low-level meridional flow between 0° N and 10° N. These results suggest the existence of a significant connection between precipitation over the southern tropical Andes and convection over the western Amazon, which is part of the meridional circulation over western tropical South America. The association between upward motion and cross-equatorial low-level northerlies in

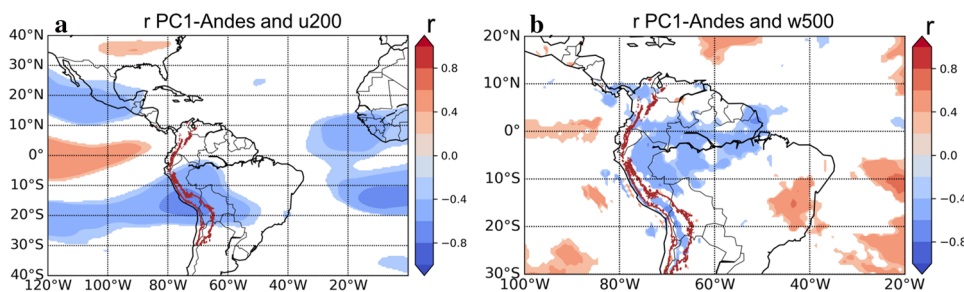


Fig. 3 **a** Correlation field between the first principal component of December–February (DJF) precipitation over the southern tropical Andes (PC1-Andes; > 3000 m.a.s.l.; 12° S– 20° S) and zonal winds at 200 hPa (U200) for the 1982–2018 period. Only correlation values

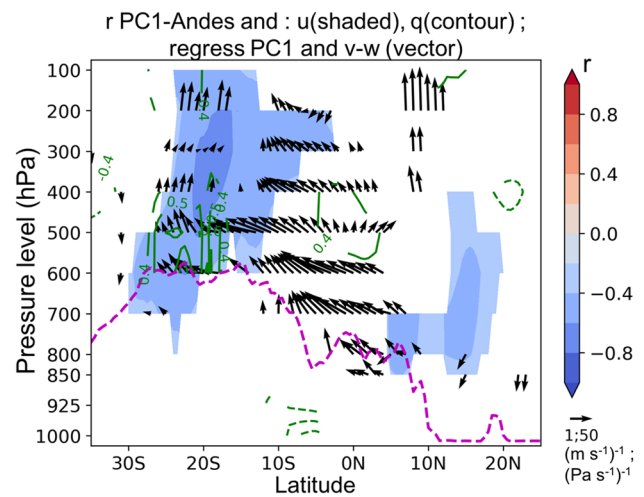


Fig. 4 Pressure-latitude cross section of the first principal component of December–February (DJF) precipitation over the southern tropical Andes (PC1-Andes; > 3000 m.a.s.l.; 12° S– 20° S) regressed upon DJF zonal-mean meridional circulation (v, w) in the tropical North Atlantic and western tropical South America. Correlation coefficients between PC1-Andes and DJF zonal-mean u (q) are shown in shaded colors (contours). Positive (negative) correlation values between PC1-Andes and q are shown in solid (dashed) contours and they have an interval of 0.1. Regression and correlation analyses are performed for the 1982–2018 period. Only significant correlation values at 95% confidence level are shown. Regression coefficients associated with meridional winds and vertical motion are shown if either the regression coefficient for the meridional or vertical component has a confidence level of 95% according to a F test. Zonal-mean is calculated using v, w, u and q in the region delimited by the magenta line in Fig. 1b. The dashed magenta line is the Andes' profile calculated as in Fig. 1c. Atmospheric data is retrieved from the ERA-Interim reanalysis data set

the tropical region was already identified in theoretical studies (Gill 1980; Silva Dias et al. 1983). However, to our best knowledge, convection over the western Amazon has not been identified in previous studies as a possible explanatory factor for precipitation variability in the southern tropical Andes. Though several studies have shown daily extreme

significant at the 95% confidence-level are shown. **b** Same as **a** but for DJF vertical motion at 500 hPa. In **a, b** the 3000 m.a.s.l. contour is shown as a crimson line. Atmospheric data are retrieved from the ERA-Interim reanalysis data set

precipitation events over the eastern tropical Andes to be tied to convection over the western Amazon, the mechanism for triggering convection was generally associated with southerly cold air incursions originating over high latitudes (Hurley et al. 2015; Sicart et al. 2016) rather than with the meridional circulation over western tropical South America as we show in this study.

As explained in Sect. 1, an intensification of convection over the Amazon since the beginning of the 21st century has been detected in several studies (Barichivich et al. 2018; Wang et al. 2018; Espinoza et al. 2019a). In the following sections, we analyze how enhanced convection over the western Amazon has influenced the long-term precipitation variability in the southern tropical Andes.

4.2 Long-term precipitation increase in the southern tropical Andes

A trend analysis shows a significant increase in PC1-Andes for the 1982–2018 period (p value < 0.05 in Kendall test). The increasing trend is still significant (p value < 0.05) when discarding the extreme values of 1983 and 1984 (not shown), which are associated with strong El Niño and La Niña events, respectively. In-situ precipitation also displays an increasing trend over the 1982–2015 period, at a 90% confidence level (p value < 0.1 ; Fig. 2c). At a regional scale, the precipitation increase for the 1982–2018 period is significant (p value < 0.05) in the northernmost regions and the western

slopes of the southern tropical Andes (Figure S1a). If we reduce the period of analysis to 1987–2018, a significant precipitation increase is also observed in the southernmost region (18°S – 20°S ; Figure S1b). In-situ precipitation also exhibits this pattern (Figure S1c,d). These results suggest a significant increase in regional December–February precipitation over the southern tropical Andes for the 1982–2018 period. In particular a reduction in the number of extreme dry years is observed (red and black lines in Fig. 2c). The decrease in extreme dry years could affect the phenology of the Altiplano flora. Indeed, Chávez et al. (2019) have demonstrated an exceptional increase in peatland productivity for the period 2002–2017 in the Altiplano using the NDVI Landsat data set.

Strengthening of the meridional circulation over western tropical South America

A trend analysis of horizontal winds at 200 hPa for the 1980–2018 period shows a significant acceleration of east-lies over the equatorial western Amazon and of westerlies over subtropical South America. On the other hand, no significant trends in zonal winds at 200 hPa are observed over the southern tropical Andes (Fig. 5a). This means that positive precipitation trends observed in the southern tropical Andes are not directly associated with changes in U200 over this region and that other possible influencing factors have to be identified. To start with, let's come back to the pioneering

Trend w500 (shaded) and u200-v200 (vectors)

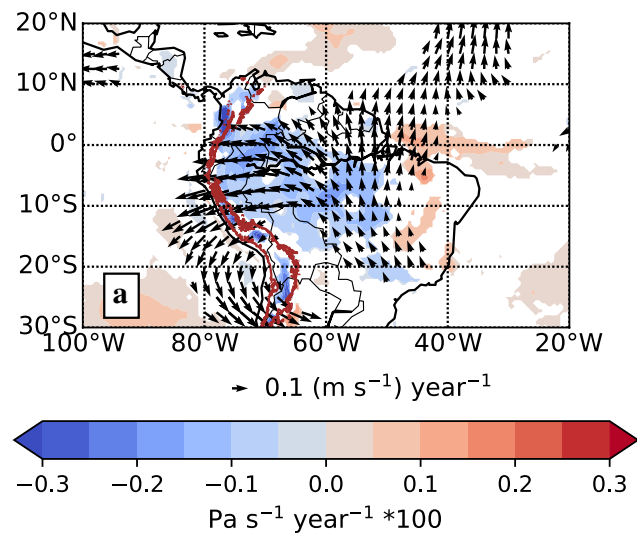
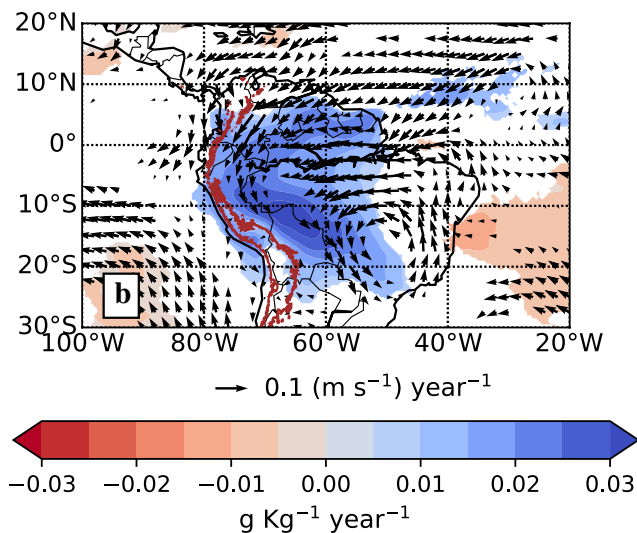


Fig. 5 a Trend analysis of December–February (DJF) vertical motion at 500 hPa (w500; shaded) and DJF horizontal winds at 200 hPa (u200–v200; vectors) calculated by using a linear regression for the 1980–2018 period. Only trends significant at the 95% confidence level according to a Kendall-test are shown. Trends in horizontal winds are shown if trends in either zonal or meridional component

Trend q500 (shaded) and u800-v800 (vectors)



are significant at 95% level. **b** Same as **a** but for specific humidity at 500 hPa (q500; shaded) and horizontal winds at 800 hPa (u800–v800). In **a**, **b** the 3000 m.a.s.l. contour is shown as a crimson line. Atmospheric data is retrieved from the ERA-Interim reanalysis data set

work of Gill (1980) and Silva Dias et al. (1983), stating that upper-level easterly acceleration in the equatorial region is explained as being a response to an intensified heat source closer to the equator. Considering the 1980–2018 tendency for the ascending motion at 500 hPa over the western Amazon, a likely candidate for providing this heating source is the associated enhanced convection in this region (Fig. 5a), already detected in previous studies (Barichivich et al. 2018; Espinoza et al. 2019a). The overall scheme would thus go as follows: intensified convection over the western Amazon has provided a heating source close to the equator, causing acceleration of the upper-level easterlies over western equatorial South America and distorting the traditional Bolivian High response.

Since convection over the western Amazon is connected to low-level northerlies, as components of the meridional circulation over western tropical South America (Fig. 4), we performed a trend analysis of horizontal winds at 800 hPa over 1980–2018 (Fig. 5b). As expected, a significant intensification of horizontal winds originating over the tropical Atlantic Ocean and directed towards the continent is observed (Fig. 5b). Figure 5b also shows an intensified low-level northerly flow to the east of the Andes between 10° S and 10° N, while eastern equatorial South America between 60° W and 40° W is characterized by intensified low-level easterlies. This low-level wind intensification coincides with an increase in specific humidity at 500 hPa, especially over the Peruvian–Bolivian Amazon (Fig. 5b), suggesting an increase in moisture transport. Monsoon theory indicates that while low-level winds transport energy and mass from

one hemisphere to the other, upper-level winds are responsible for balancing the energy and mass budget by maintaining mass and energy transport in the opposite direction of the low-level meridional winds. This process is observed in Fig. 5a, in which intensified southerlies at 200 hPa are observed crossing the equator between 60° W and 40° W. These results are also found using the NCEP-NCAR reanalysis (Figure S2), indicating that this is a robust feature across different reanalysis products.

Figure 6a shows that the zonal-mean atmospheric circulation in western tropical South America was significantly strengthened during the 1980–2018 period. In general, we observe an intensification of the ascending branch, located over the western Amazon (15° S–0° N), and an increased low-level northerly flow between 10° S and 20° N. This mechanism is explained by the transient solution presented in Silva Dias et al. (1983). As the heat source intensifies closer to the equator, the upper-level high drifts to the southwest of the heat source and the baroclinic response leads to a northerly flow acceleration in the lower troposphere. The latter suggests an enhanced moisture transport from the tropical North Atlantic towards the western Amazon, which would explain the significant increase in specific humidity at levels from 850 to 100 hPa in the region of the ascending branch. It is known that reanalysis products have problems in reproducing the cross-equatorial mass flux—even though ERA-Interim reanalysis are performing the best in this respect (Berrisford et al. 2011)—casting some uncertainty on the quantitative results of our analysis. However, the strengthening of the meridional circulation over western tropical South

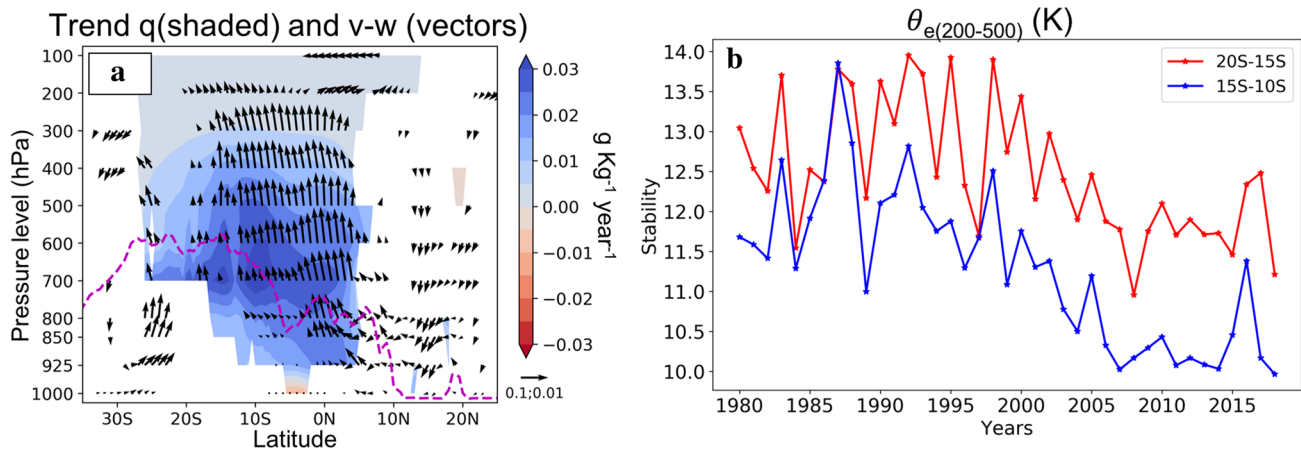


Fig. 6 **a** Pressure-latitude cross-section of trends in DJF zonal-mean meridional circulation (v–w, vectors) and specific humidity (shaded) in the tropical North Atlantic and western tropical South America. Linear trends are calculated using a linear regression for the 1980–2018 period and only significant values at the 95% confidence-level according to a Kendall-test are shown. Vectors are shown if trend in either the meridional or vertical component is significant at the 95% confidence level. Zonal-mean is calculated as explained in Fig. 1c.

The dashed magenta line shows the Andes' profile calculated as in Fig. 1c. **b** Interannual time series of December–February stability index ($\theta_{e(200-500)}$) in the 20° S–15° S region (red line) and in the 15° S–10° S region (blue line) between 80° W–60° W, excluding zones to the west of the Andes as shown in Fig. 1b. $\theta_{e(200-500)}$ is calculated as the difference between equivalent potential temperature at 200 hPa and 500 hPa for the period 1980–2018. Atmospheric data is retrieved from the ERA-Interim reanalysis data set

America identified in our study is consistent with the theoretical response to an equatorial diabatic heat source (Gill 1980; Silva Dias et al. 1983). Furthermore, positive trends in precipitation and streamflow over the western Amazon, associated with intensified convection over this region, have already been documented in previous studies (Barichivich et al. 2018; Wang et al. 2018; Espinoza et al. 2019a).

Positive trends in specific humidity are observed in the mid-troposphere (700–500 hPa), indicating that vertical moisture transport from the lower to the mid-troposphere has intensified over the 1980–2018 period (Fig. 6a). In the Amazon, the seasonal increase in mid-tropospheric moisture, which results in an increased equivalent potential temperature (θ_e) at mid-tropospheric levels, is associated with the development of deep convection over this region due to reduced atmospheric stability between the mid- and upper troposphere (Fu et al. 1999; Scala et al. 2008; Zhuang et al. 2017). Due to the mid-tropospheric moistening over western tropical South America (80° W–60° W) since 1980, we also observe an increased θ_e at this tropospheric level (not shown). Furthermore, the difference of equivalent potential temperature (θ_e) between 200 and 500 hPa ($\theta_{e(200-500)}$) over western tropical South America between 20° S and 15° S indicates a strong reduction in atmospheric stability between the mid and the upper troposphere in the southern tropical Andes since 2000 (Fig. 6b). Indeed, highest atmospheric stability values after 2000 are similar to the lowest values in the period before 2000. Atmospheric stability in western tropical South America between 15° S and 10° S also shows a reduction, but it starts at the beginning of the 1990s (Fig. 6b). Thus, atmospheric stability between the mid- and the upper troposphere is no longer a restriction for developing convection not only over the western Amazon, but also over the southern tropical Andes. The decrease in atmospheric stability could explain the reduction in the number of dry years in this Andean region as shown in Fig. 2c. Furthermore, the decreased atmospheric stability observed in the western Amazon seems to be concomitant with the detected precipitation trend in northern regions of the southern tropical Andes.

Hsu et al. (2012) argued that a future precipitation increase in monsoon regions is due to tropospheric moistening (thermodynamic component)—linked to a warming of the tropical oceans—rather than changes in the atmospheric circulation in the tropics, especially changes in wind convergence (dynamic component). For the 1982–2018 period, we found results over tropical South America that are consistent with that vision. In particular, we found a spatial pattern of the vertically integrated total moisture trends in the troposphere (1000–100 hPa; not shown) that is similar to the spatial pattern of the 500 hPa specific humidity trends displayed in Fig. 5b, while no significant trends are observed in vertically integrated wind convergence (not shown).

Hence, these results indicate that observed positive trends in precipitation in the southern tropical Andes are significantly associated with increased convection over the Amazon and reduced atmospheric stability over the southern tropical Andes. These processes are connected with an increased vertical moisture transport from lower- to upper-tropospheric levels over western tropical South America. In the next section, we will show how the relationship between precipitation over the southern tropical Andes and atmospheric circulation over the western Amazon has concomitantly evolved with time for the 1982–2018 period.

4.3 Long-term variation in the interannual precipitation variability

In the previous section, we showed that atmospheric stability over western tropical South America south of 10° S has been reduced. At the same time, it appears from Fig. 6b that its year-to-year variability has also been reduced after 2006, suggesting a more constant vertical moisture transport from the lower to the mid-troposphere over those regions, including the southern tropical Andes. This raises the question whether the strengthening of the meridional circulation, through constant vertical moisture transport and a more predisposed atmosphere to develop deep convection, has affected the year-to-year precipitation variability in the southern tropical Andes, thereby becoming its principal source of interannual variability.

As seen previously, PC1-Andes has an intrinsic significant decadal trend, which is associated with the strengthening of the meridional circulation over western tropical South America. Figure 7a shows that PC1-Andes also exhibits a decadal fluctuation, but since it only covers 37 years (1982–2018) it is difficult to evaluate its significance. It is, however, necessary to filter out this decadal-scale signal in order to retrieve the interannual signal and examine its linkage with the fluctuation of the meridional circulation. To that end, a high-pass filter was applied to PC1-Andes with a cutoff period of 8 years (see Sect. 3.2.2). The time series associated with the interannual PC1-Andes variability is referred to as PC1-high (black line in Fig. 7a). The removal of the decadal-scale signal was equally applied to vertical and horizontal winds and specific humidity for the same region shown in Fig. 4, in order to obtain their interannual fluctuations. PC1-high is then regressed upon the zonal-mean meridional wind and vertical motion over western tropical South America and the tropical North Atlantic at different tropospheric levels (1000–100 hPa; Fig. 7b). Figure 7b also shows a correlation analysis between PC1-high and the zonal-mean specific humidity and zonal winds. This analysis is similar to the one carried out in Fig. 4, in which unfiltered data were used.

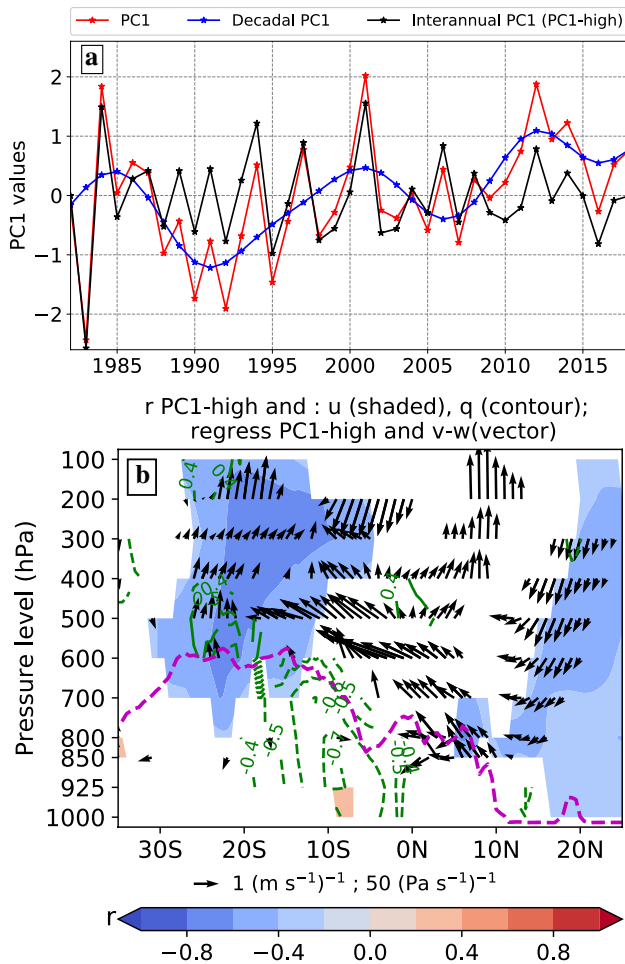


Fig. 7 **a** First principal component of December–February precipitation over the southern tropical Andes (PC1-Andes; red line), its interannual variability as PC1-high (periodicity < 8 years; black line) and its decadal variability (periodicity > 8 years; blue line). **b** As in Fig. 4, except for PC1-high and interannual variations (periodicity < 8 years) of specific humidity, zonal and meridional winds and vertical motion in the tropical North Atlantic and western tropical South America

Significant regression coefficients are observed between PC1-high and vertical motion above 600 hPa in the western Amazon, similar to the results using unfiltered data (Fig. 4), suggesting that convection over the western Amazon is significantly associated with precipitation over the southern tropical Andes at interannual time scales for the 1982–2018 period. Figure 7b displays significant correlation values between PC1-high and zonal wind in the mid- and the upper troposphere over western tropical South America between 25° S and 15° S. Aside from the significant positive relationship with specific humidity over the southern Altiplano, PC1-high also shows a significant negative correlation with specific humidity in the mid- and the lower troposphere between 20° S and 0° N (Fig. 7b). Thus, at interannual time scales, positive

anomalies of lower-tropospheric moisture over the western Amazon are associated with a precipitation decrease in the southern tropical Andes, maybe due to a decreased upward moisture transport from the western Amazonian lowlands.

Since a strengthening of the meridional circulation over western tropical South America has been observed for the 1982–2018 period, we next explore whether the influence of western Amazon convection and upper-level zonal winds on southern tropical Andes precipitation have changed over time at interannual time scales. We performed a correlation analysis using different time periods and window lengths between PC1-high and the interannual fluctuations of vertical motion at 500 hPa (w500-high) in two regions of western tropical South America (80° W–60° W): 20° S–15° S (Fig. 8a) and 15° S–10° S (Fig. 8b). Correlation coefficients are displayed in Fig. 8 as a function of the length of the correlation period in years (y-axis) and the last year of this period (x-axis), meaning that correlation coefficients were analyzed for all possible time periods. For instance, the correlation value at point $x = 1998, y = 10$ indicates that the correlation analysis is carried out for a time period of 10 years ending in 1998 (1989–1998). w500-high in 20° S–15° S represents an average of vertical velocities at 500 hPa between the northern Altiplano and the western Amazonian lowlands. For the region in 15° S–10° S, w500-high mainly corresponds to vertical velocities at 500 hPa over the western Amazon. This analysis is also done using the interannual variability of zonal winds at 200 hPa in the region between 20° S and 15° S of western tropical South America (U200-Andes; Fig. 8c).

It is evident in Fig. 8 that w500-high in regions 20° S–15° S (Fig. 8a) and 15° S–10° S (Fig. 8b) has undergone a change in its relationship with PC1-high. Before 2002, both regions show a positive but insignificant correlation between w500-high and PC1-high. After 2002, this relationship has become negative and significant (p value < 0.05), meaning that intensified upward motion over the western Amazon is associated with more precipitation over the southern tropical Andes at interannual time scales. A different pattern is observed in the correlation analysis between PC1-high and U200-Andes (Fig. 8c). U200-Andes over this Andean sub-region is significantly correlated with PC1-high before 2002, while for the period 2002–2018 no significant correlation is observed. Indeed, a significant correlation coefficient between PC1-high and U200-Andes is observed for the 1982–2018 period (upper right in Fig. 8c) mostly due to strong correlation values between these two variables before 2002. Hence, U200-Andes and interannual variations of vertical velocities at 500 hPa in 15° S–10° S, denoted as w500-Amazon, are the principal atmospheric mechanisms that explain the interannual variability of precipitation over the southern tropical Andes, but their respective influence has changed over the 1982–2018 period.

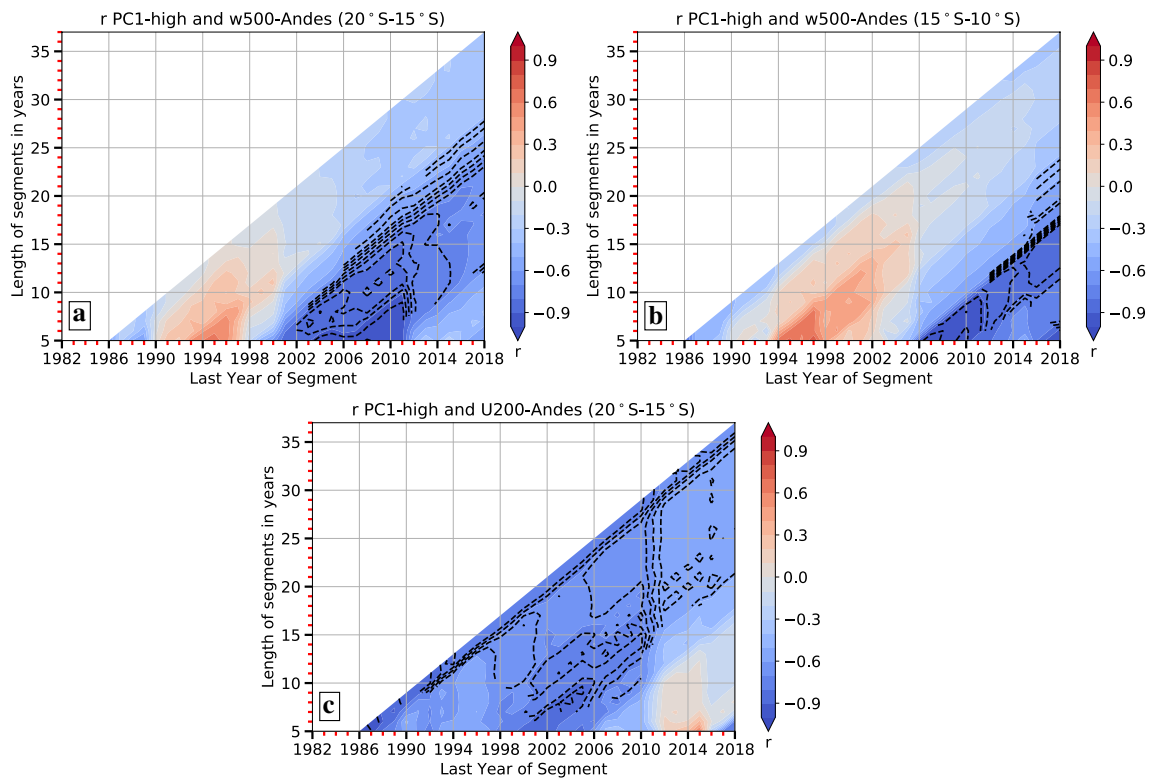


Fig. 8 **a** Correlation analysis between PC1-high and interannual fluctuations (periodicity < 8 years) of DJF vertical motion at 500 hPa (w500-high) in the region 80° W–60° W; 20° S–15° S. Correlation coefficients are shown as a function of the length of analyzed period in years (y-axis) and the ending year of the analyzed period (x-axis). Contours indicate segments with significant correlation values at 95% confidence level. **b** similar to **a** but using w500-high in the region

80° W–60° W; 15° S–10° S. **c** similar to **a** but for interannual fluctuations of DJF zonal wind at 200 hPa in the region 80° W–60° W; 20° S–15° S (U200-Andes). Vertical motion at 500 hPa and zonal wind at 200 hPa are calculated excluding zones to the west of the Andes as shown in Fig. 1b. Atmospheric data is retrieved from the ERA-Interim reanalysis data set

A correlation analysis between w500-Amazon and U200-Andes yields a correlation coefficient of $r = 0.33$ (p value < 0.05). Although the correlation between w500-Amazon and U200-Andes is significant, the low correlation coefficient indicates that these variables are only weakly related since they share only 10% of the variance. In addition, this result suggests that the regional atmospheric circulation associated with U200-Andes and w500-Amazon is different. With the aim of identifying atmospheric mechanisms associated with U200-Andes and w500-Amazon, we performed a correlation analysis using these two variables and interannual variations (< 8 years) of zonal-mean zonal winds and specific humidity at different tropospheric levels over western tropical South America and the tropical North Atlantic (Fig. 9). The regression analysis between the interannual variability of the meridional circulation (meridional wind and vertical motion) over these regions and both U200-Andes and w500-Amazon is also shown in Fig. 9. These analyses are done for the 1980–2018 period. Since U200-Andes and w500-Amazon are negatively correlated with PC1-high, we multiplied U200-Andes and w500-Amazon by

-1 before computing the correlation and regression analyses. Our objective with this procedure is to obtain atmospheric circulation associated with upper-level easterlies over the Altiplano (U200-Andes \times -1) and upward motion over the western Amazon (w500-Amazon \times -1), indices of the two mechanisms that enhance precipitation over the southern tropical Andes.

As expected, negative values of U200-Andes (easterlies) are associated with easterly anomalies above 600 hPa between 25° S and 15° S (Fig. 9a). This correlation pattern is related to the vertical structure of the Bolivian High, shown by Lenters and Cook (1997). Figure 9a also shows that negative values of U200-Andes (easterlies) are not related to upward motion on a regional scale, but on a local scale, especially in the southern Altiplano. In addition, a moistened mid-troposphere in this region is associated with negative U200-Andes values (easterlies). A different correlation pattern is found when using negative values of w500-Amazon (Fig. 9b). Negative w500-Amazon values (upward motion) are characterized by a significant relationship with lower and mid-tropospheric upward flow between 20° S and 10° S.

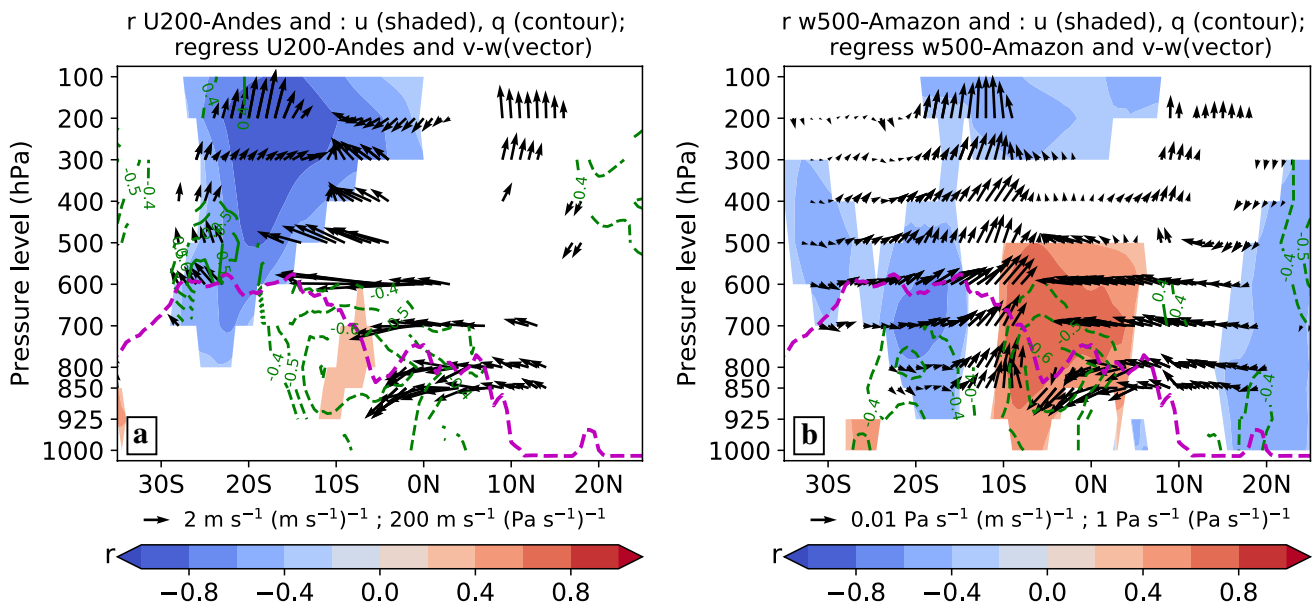


Fig. 9 **a** Pressure-latitude cross section of December–February (DJF) zonal winds at 200 hPa (U200) in the region 80° W–60° W; 20° S–15° S regressed upon DJF zonal-mean meridional circulation (v,w) in the tropical North Atlantic and western tropical South America at interannual time scales (periodicity < 8 years). The interannual time series of DJF U200 in the region 80° W–60° W; 20° S–15° S is referred as U200-Andes. Zones to the west of the Andes between 20° S and 15° S, as shown in Fig. 1b, are excluded when computing U200-Andes. Moreover, U200-Andes has been multiplied by -1 (easterlies pattern). Correlation coefficients between U200-Andes and interannual fluctuation of zonal-mean u (q) are shown in shaded colors (contours). Positive (negative) correlation values between negative U200-Andes, easterlies pattern, and q are shown in solid (dashed) contours and they have an interval of 0.1. Regression and

correlation analyses are computed for the 1980–2018 period. Only significant correlation values at 95% confidence level are shown. Regression coefficients associated with meridional wind and vertical motion are shown if regression coefficients for either the meridional or vertical component show a confidence level of 95% according to a F test. **b** similar to **a**, but instead of U200-Andes, the interannual variability of vertical motion at 500 hPa in the region 15° S–10° S; 80° W–60° W (w500-Amazon) is used. Zones to the west of the Andes between 15° S and 10° S, as shown in Fig. 1b, are excluded when computing w500-Amazon. In **a**, **b** zonal-mean u , v , q and w are calculated as explained in Fig. 1c. In **a**, **b** the dashed magenta line represents the Andes' profile calculated as in Fig. 1c. Atmospheric data is retrieved from the ERA-Interim reanalysis data set

Figure 9b also shows that w500-Amazon is associated with anomalous low- and mid-level northerlies between 5° S and 20° N and low- and mid-level westerly anomalies at the Equator. Accordingly, convection over the western Amazon between 15° S and 10° S at interannual time scales (periodicity < 8 years) is sustained by increased low- and mid-level moisture transport from the tropical North Atlantic rather than moisture transport originating over eastern equatorial South America. An interesting feature regarding Fig. 9 is the relationship between decreased lower-tropospheric moisture between 20° S and 0° N, associated with negative values of U200-Andes (Fig. 9a) and w500-Amazon (Fig. 9b). Thus, at interannual time scales, upper-level easterlies over the Altiplano between 20° S and 15° S are associated with local convection over this region and horizontal moisture transport towards the southern tropical Andes from the central Amazon. On the other hand, upward motion over the western Amazon (15° S–10° S) is associated with a regional increase in vertical moisture transport from lower- to upper-tropospheric levels, especially in the region between 20° S and 10° S. These results are explained using Gill's model

(Gill 1980) and the results of Silva Dias et al. (1983). U200-Andes is more closely related to the convective forcing in the continental portion of the SACZ while the meridional flow is very much influenced by the equatorial heat source in the western Amazon. Thus, when convection over the western Amazon is enhanced, cross-equatorial northerly winds in the lower troposphere are accelerated. Moreover, Silva Dias et al. (1983) showed that an equatorial heat source could perturb upper-level easterlies in the equatorial region but not in the southwest region of the heating.

As previously described, interannual variations in precipitation over the southern tropical Andes respond differently to U200-Andes and w500-Amazon after 2002 (Fig. 8b, c). In order to identify significant patterns of atmospheric circulation associated with precipitation over the southern tropical Andes at interannual time scales, we performed a correlation analysis similar to the one shown in Fig. 6a, but, in this case, the correlation was done for two periods: 1982–2001 (Fig. 10a) and 2002–2018 (Fig. 10b). For the 1982–2001 period, PC1-high is significantly correlated with zonal winds above the Altiplano (Fig. 10a), and the correlation pattern is

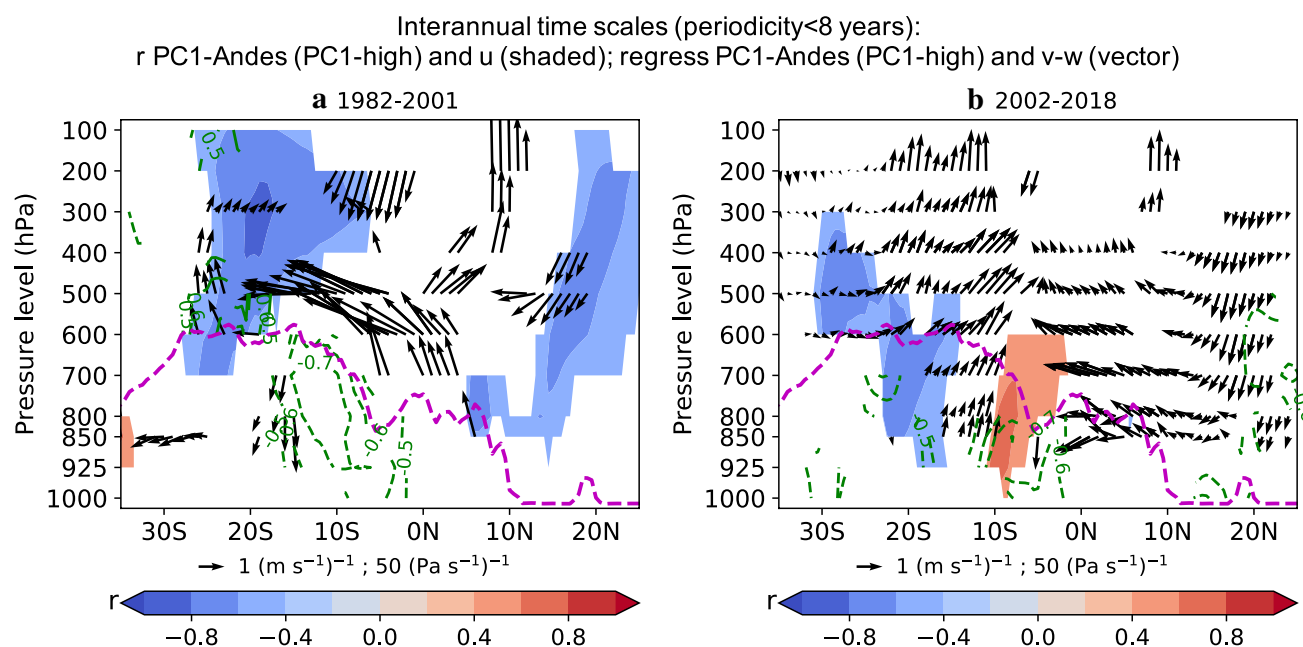


Fig. 10 Similar to Fig. 6a but for **a** the 1982–2001 period and **b** the 2002–2018 period

similar to atmospheric circulation associated with negative values of U200-Andes (easterlies; Fig. 9a). The correlation analysis for the period 2002–2018 shows a different pattern, where upper-level zonal winds over the Altiplano are no longer significantly associated with PC1-high (Fig. 10b). Instead, PC1-high is significantly correlated with vertical velocities between 20° S and 10° S, especially above 600 hPa, and with meridional winds in the mid- and the lower troposphere (850–600 hPa) in the Northern Hemisphere (north of 0° N; Fig. 10b). The similarities between Fig. 9b and 10b lead us to conclude that the pattern of interannual variability of December–February precipitation over the southern tropical Andes for the 2002–2018 period is strongly influenced by enhanced convection over the western Amazon and increased low-level moisture transport from the tropical North Atlantic.

5 Discussion and conclusions

The results presented above led us to propose a schematic (Fig. 11) where the two main elements of the atmospheric circulation controlling December–February (DJF) precipitation over the southern tropical Andes (20° S–12° S and > 3000 m.a.s.l.) are represented. The mechanisms by which these two elements exercise their control are summarized below, as is the evolution of their influence over the last 35 years.

The first element is the zonal wind at 200 hPa (U200). Previous studies (e.g. Vuille et al. 1998; Garreaud et al.

2003; Vuille and Keimig 2004; Garreaud 2009; Vera et al. 2019) have demonstrated that a strong negative relationship exists between DJF precipitation and U200 over the southern tropical Andes (i.e., high values of DJF precipitation are associated with stronger easterlies at 200 hPa) at different time scales. U200 over this Andean region is part of the so-called Bolivian High, which is indeed a response to the latent heat release generated by deep convection over the continental region of the South Atlantic Convergence Zone—SACZ (Silva Dias et al. 1983; DeMaria 1985; Figueroa et al. 1995; Lenters and Cook 1997; Gandu and Silva Dias 1998; Rodwell and Hoskins 2001). This U200-related mechanism (schematized in Fig. 11 in red color) does not show any significant change over the 1980–2018 period; yet, DJF precipitation displays a significant increase over the same period. This suggests another controlling mechanism that took over since the beginning of the 2000's.

This second controlling mechanism is the upward motion over the western Amazon—which is part of the meridional circulation between the tropical North Atlantic and western tropical South America (blue color in Fig. 11). This upward motion over the western Amazon has intensified over the two last decades as part of the increased meridional moisture transport from the tropical North Atlantic. This led to increased convection and reduced atmospheric stability between the mid- and upper troposphere over western tropical South America, including the southern tropical Andes, resulting in increased moisture transport from lower- to mid-tropospheric levels. These results are in line with the theory proposed in Gill (1980) and Silva Dias et al. (1983). Indeed,

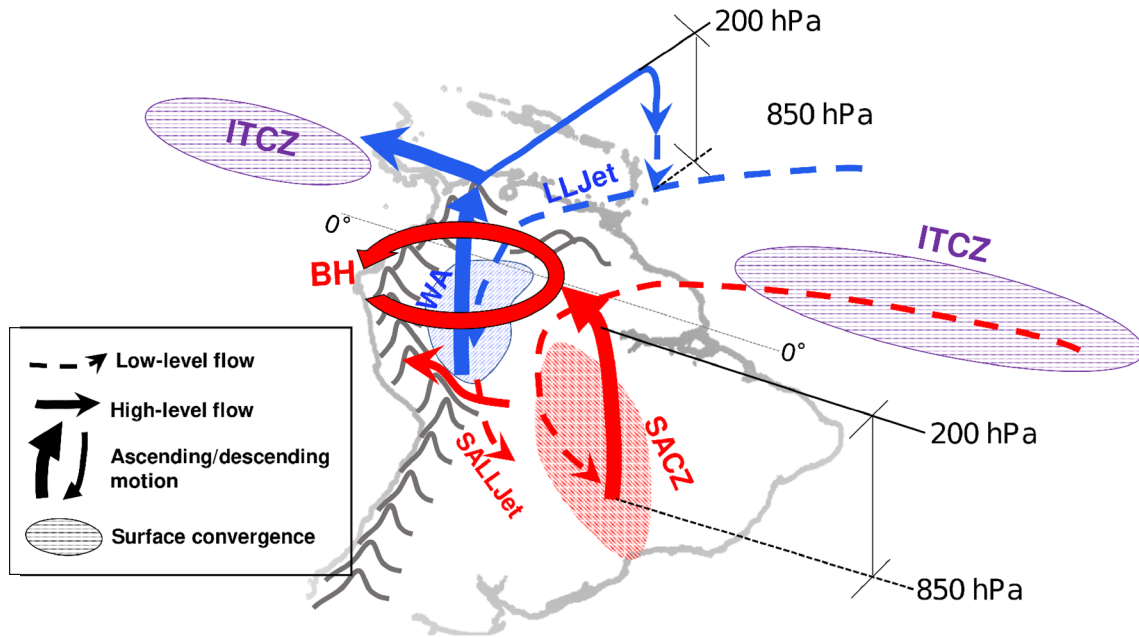


Fig. 11 Schematic representation of the two atmospheric mechanisms controlling the December–February (DJF) precipitation over the southern tropical Andes. The first mechanism (in red) is the moisture-laden near-surface upslope flow at the eastern side of the southern tropical Andes. This mechanism is associated with the so-called Bolivian High (BH), developed by deep convection over the continental South Atlantic Convergence Zone (SACZ). Moisture transport towards the SACZ is controlled by the South American Low-Level Jet (SALLJet) and the low-level flow from the tropical Atlantic Ocean,

including the Intertropical Convergence Zone (ITCZ). The second mechanism (in blue) is the upward motion over the western Amazon (WA), which is an important factor for decreasing atmospheric stability over the southern tropical Andes. Upward motion over the WA and the Llanos Low-Level Jet (LLJet) are components of the meridional circulation between the tropical North Atlantic and western tropical South America. Upper-level easterlies over western equatorial South America are also associated with this meridional circulation

while upper-level easterly acceleration over the southern tropical Andes is associated with diabatic heating south of the equator (continental SACZ), the cross-equatorial

wind acceleration in the lower and upper troposphere is a response of a more equatorial heat source provided by the enhanced convection over the western Amazon. This latter

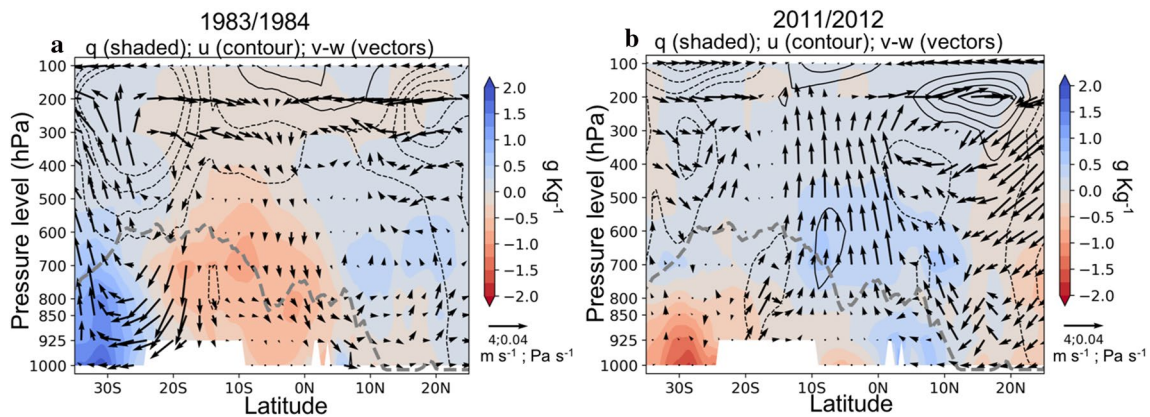


Fig. 12 a Anomalies of zonal-mean December–February (DJF) specific humidity (q ; shaded), zonal winds (u , contours), meridional winds and vertical motion ($v-w$; vectors) in 1983/1984. Positive anomalies of zonal wind are shown in solid (dashed) contours and the interval between contours is 2 m s^{-1} . The contour of 0 m s^{-1} is omitted

for zonal winds. **b** similar to **a** but for 2011/2012. In **a, b** zonal-mean is calculated as explained in Fig. 1c. In **a, b** dashed gray line represents the Andes' profile calculated as in Fig. 1c. Atmospheric data is retrieved from ERA-Interim reanalysis data set

enhancement of convection over the western Amazon was identified in previous studies (Barichivich et al. 2018; Wang et al. 2018; Espinoza et al. 2019a).

The hypothesis of the existence of two atmospheric mechanisms determining the DJF precipitation variability over the southern tropical Andes, U200 and western Amazon convection, is favored by the analysis of its interannual variability (periodicity < 8 years) and its associated atmospheric mechanisms. Before 2000, a period when upward motion over the western Amazon was not strong enough for decreasing atmospheric stability, the interannual variability of DJF precipitation was strongly coupled with U200 over the southern tropical Andes, because easterly anomalies aloft favored moist air transport towards the central Andes, where dry conditions would otherwise prevail. Besides, strong moisture transport from the interior of the continent associated with upper-level easterly anomalies was often connected with La Niña summers. For instance, high DJF precipitation values in the southern tropical Andes during the 1983/1984 La Niña year was associated with upper-level easterly anomalies above the southern tropical Andes and anomalous subsidence over the western Amazon (Fig. 12a). From 2000 to 2002 onwards, a regional analysis evidences that interannual fluctuations of southern tropical Andes precipitation started to be significantly associated with the meridional circulation over western tropical South America. Thus, enhanced convection over the western Amazon and strengthened low-level northerlies originating over the tropical North Atlantic seem to explain anomalous wet years in the southern tropical Andes after 2002, as occurred during the 2011/2012 La Niña summer (Fig. 12b). As a matter of fact, the low-level northerly flow has been identified as being the cause of anomalous wet years in the northwestern Amazon (Espinoza et al. 2013; Arias et al. 2015).

The existence of these two independent modes challenges our vision of how global change might impact the regional rainfall regime. Whilst, up to now, the role of U200 anomalies has been emphasized (Garreaud et al. 2003; Minvielle and Garreaud 2011; Neukom et al. 2015; Vera et al. 2019) as the main driver of past and future precipitation changes in this region, changing conditions over the western Amazon and warming of the tropical North Atlantic could also play a major role in shaping the long-term evolution of precipitation in the southern tropical Andes. Indeed, the projected decrease in summer precipitation in the Altiplano—due to westerly acceleration of the upper-level winds over the Andes—can be offset by an increase in western Amazon convection, an issue that deserves further scrutiny. By the same token, this explains why the use of ENSO for predicting southern tropical Andes rainfall is not as powerful as it once appeared, since its influence is modulated by these two competing regional circulation factors. These results pave

the way for considering new research topics, such as the influence of western Amazon convection on the variability of southern tropical Andes precipitation on a larger spectrum of time scales, ranging from diurnal, to intraseasonal, seasonal and decadal.

Acknowledgements This research was funded by the IDEX grants of University Grenoble Alpes (UGA), the VASPAT project IDEX “IRS-Initiative de Recherche Stratégique” (part of the ANR project ANR-15-IDEX-02) of UGA and the French AMANECER-MOPGA project funded by ANR and IRD (ref. ANR-18-MPGA-0008). Authors from IGE acknowledge the support of the Labex OSUG@2020 (Investissements d’avenir-ANR10 LABX56). We thank to the CYME team of IGE for constant exchange of ideas that have improved the quality of the research. We give special thanks to J. Ronchail and L. Li of IPSL for their contributions in the framework of H. Segura’s PhD. thesis committee. Finally, we are very grateful to the reviewers because their comments have improved the quality of our study.

References

- Aceituno P, Garreaud R (1995) Impacto de los fenómenos el Niño y la Niña en regímenes fluviométricos andinos. *Rev Soc Chil Hidrául* 10(2):33–43
- Adler RF, Huffman GJ, Chang A, Ferraro R, Xie PP, Janowiak J, Rudolf B, Schneider U, Curtis S, Bolvin D, Gruber A, Susskind J, Arkin P, Nelkin E (2003) The version-2 global precipitation climatology project (GPCP) monthly precipitation analysis (1979–Present). *J Hydrometeorol* 4(6):1147–1167
- Adler RF, Sapiano MR, Huffman GJ, Wang JJ, Gu G, Bolvin D, Chiu L, Schneider U, Becker A, Nelkin E, Xie P, Ferraro R, Shin DB (2018) The Global Precipitation Climatology Project (GPCP) monthly analysis (New Version 2.3) and a review of (2017) global precipitation. *Atmosphere (Basel)* 9:4. <https://doi.org/10.3390/atmos9040138>
- Allan RP, Soden BJ, John VO, Ingram W, Good P (2010) Current changes in tropical precipitation. *Environ Res Lett* 5:2. <https://doi.org/10.1088/1748-9326/5/2/025205>
- Arias PA, Martínez JA, Vieira SC (2015) Moisture sources to the 2010–2012 anomalous wet season in northern South America. *Clim Dyn* 45(9–10):2861–2884. <https://doi.org/10.1007/s00382-015-2511-7>
- Barichivich J, Gloor E, Peylin P, Brienen RJW, Schöngart J, Espinoza JC, Pattayak KC (2018) Recent intensification of Amazon flooding extremes driven by strengthened Walker circulation. *Sci Adv* 4(9):8785. <https://doi.org/10.1126/sciadv.aat8785>
- Bendix J, Lauer W (1992) Die Niederschlagsjahreszeiten in Ecuador und ihre klimadynamische Interpretation (Rainy Seasons in Ecuador and Their Climate-Dynamic Interpretation). *Erdkunde* 2(1992):118–134. <http://www.jstor.org/stable/25646379>
- Berntell E, Zhang Q, Chafik L, Körnich H (2018) Representation of multidecadal Sahel rainfall variability in 20th century reanalyses. *Sci Rep* 8(1):6–13. <https://doi.org/10.1038/s41598-018-29217-9>
- Berrisford P, Källberg P, Kobayashi S, Dee D, Uppala S, Simmons AJ, Poli P, Sato H (2011) Atmospheric conservation properties in ERA-Interim. *Q J R Meteorol Soc* 137(659):1381–1399. <https://doi.org/10.1002/qj.864>
- Bordoni S, Schneider T (2008) Monsoons as eddy-mediated regime transitions of the tropical overturning circulation. *Nat Geosci* 1(8):515–519. <https://doi.org/10.1038/ngeo248>

- Chávez RO, Christie DA, Olea M, Anderson TG (2019) A multiscale productivity assessment of high Andean Peatlands across the Chilean Altiplano using 31 years of landsat imagery. *Remote Sens* 11(24):2955. <https://doi.org/10.3390/rs11242955>
- Debortoli SN, Dubreuil V, Funatsu B, Delahaye F, de Oliveira CH, Rodrigues-Filho S, Saito CH, Fetter R (2015) Rainfall patterns in the Southern Amazon: a chronological perspective (1971–2010). *Clim Change* 132(2):251–264. <https://doi.org/10.1007/s10584-015-1415-1>
- Dee DP, Uppala SM, Simmons AJ, Berrisford P, Poli P, Kobayashi S, Andrae U, Balmaseda MA, Balsamo G, Bauer P, Bechtold P, Beljaars AC, van de Berg L, Bidlot J, Bormann N, Delsol C, Dragani R, Fuentes M, Geer AJ, Haimberger L, Healy SB, Hersbach H, Hólm EV, Isaksen I, Kållberg P, Köhler M, Matricardi M, McNally AP, Monge-Sanz BM, Morcrette JJ, Park BK, Peubey C, de Rosnay P, Tavolato C, Thépaut JN, Vitart F (2011) The ERA-Interim reanalysis: configuration and performance of the data assimilation system. *Q J R Meteorol Soc* 137(656):553–597. <https://doi.org/10.1002/qj.828>
- DeMaria M (1985) Linear response of a stratified tropical atmosphere to convective forcing. *J Atmos Sci* 42(18):1944–1959. [https://doi.org/10.1175/1520-0469\(1985\)042%3c1944:LROAS%3e2.0.CO;2](https://doi.org/10.1175/1520-0469(1985)042%3c1944:LROAS%3e2.0.CO;2)
- Espinoza JC, Ronchail J, Frappart F, Lavado W, Santini W, Guyot JL (2013) The major floods in the Amazonas River and Tributaries (Western Amazon Basin) during the 1970–2012 Period: a focus on the 2012 flood*. *J Hydrometeorol* 14(3):1000–1008. <https://doi.org/10.1175/jhm-d-12-0100.1>
- Espinoza JC, Chavez S, Ronchail J, Junquas C, Takahashi K, Lavado W (2015) Rainfall hotspots over the southern tropical Andes: spatial distribution, rainfall intensity, and relations with large-scale atmospheric circulation. *Water Resour Res* 51(5):3459–3475. <https://doi.org/10.1002/2014WR016273>
- Espinoza JC, Segura H, Ronchail J, Drapeau G, Gutierrez-Cori O (2016) Evolution of wet-day and dry-day frequency in the western Amazon basin: relationship with atmospheric circulation and impacts on vegetation. *Water Resour Res* 52(11):8546–8560. <https://doi.org/10.1002/2016WR019305>
- Espinoza JC, Ronchail J, Marengo J, Segura H (2019a) Contrasting North–South changes in Amazon wet-day and dry-day frequency and related atmospheric features (1981–2017). *Clim Dyn*. <https://doi.org/10.1007/s00382-018-4462-2>
- Espinoza JC, Sorensson AA, Ronchail J, Molina J, Segura H, Gutierrez O, Ruscica R, Condom T, Wongchuig S (2019b) Regional hydro-climatic changes in the Southern Amazon Basin (Upper Madeira Basin) during the 1982–2017 period. *J Hydrol Reg Stud* 26(September):100637. <https://doi.org/10.1016/j.ejrh.2019.100637>
- Falvey M, Garreaud RD (2005) Moisture variability over the South American Altiplano during the South American low level jet experiment (SALLJEX) observing season. *J Geophys Res Atmos* 110(22):1–12. <https://doi.org/10.1029/2005JD006152>
- Figueroa SN, Satyamurty P, Da Silva Dias PL (1995) Simulations of the summer circulation over the South American Region with an eta coordinate model. *J Atmos Sci* 52(10):1573–1584. [https://doi.org/10.1175/1520-0469\(1995\)052%3c1573:SOTSC%3e2.0.CO;2](https://doi.org/10.1175/1520-0469(1995)052%3c1573:SOTSC%3e2.0.CO;2)
- Fu R, Zhu B, Dickinson RE (1999) How do atmosphere and land surface influence seasonal changes of convection in the tropical Amazon? *J Clim* 12(51):1306–1321. [https://doi.org/10.1175/1520-0442\(1999\)012%3c1306:HDAALS%3e2.0.CO;2](https://doi.org/10.1175/1520-0442(1999)012%3c1306:HDAALS%3e2.0.CO;2)
- Fu R, Yin L, Li W, Arias PA, Dickinson RE, Huang L, Chakraborty S, Fernandes K, Liebmann B, Fisher R, Myneni RB (2013) Increased dry-season length over southern Amazonia in recent decades and its implication for future climate projection. *Proc Natl Acad Sci* 110(45):18110–18115. <https://doi.org/10.1073/pnas.1302584110>
- Funk C, Peterson P, Landsfeld M, Pedreros D, Verdin J, Shukla S, Husak G, Rowland J, Harrison L, Hoell A, Michaelsen J (2015) The climate hazards infrared precipitation with stations—a new environmental record for monitoring extremes. *Sci Data* 2:150066. <https://doi.org/10.1038/sdata.2015.66>. <http://www.nature.com/articles/sdata201566>. <http://arxiv.org/abs/1011.1669v3>
- Gandu AW, Silva Dias PL (1998) Impact of tropical heat sources on the South American tropospheric upper circulation and subsidence. *J Geophys Res Atmos* 103(D6):6001–6015. <https://doi.org/10.1029/97JD03114>
- Garreaud R, Vuille M, Clement AC (2003) The climate of the Altiplano: observed current conditions and mechanisms of past changes. *Palaeogeogr Palaeoclimatol Palaeoecol* 194(1–3):5–22. [https://doi.org/10.1016/S0031-0182\(03\)00269-4](https://doi.org/10.1016/S0031-0182(03)00269-4)
- Garreaud RD (1999) Multiscale analysis of the summertime precipitation over the Central Andes. *Mon Weather Rev* 127:901–921. [https://doi.org/10.1175/1520-0493\(1999\)127%3c0901:MAOTS%3e2.0.CO;2](https://doi.org/10.1175/1520-0493(1999)127%3c0901:MAOTS%3e2.0.CO;2)
- Garreaud RD (2000) Intraseasonal variability of moisture and rainfall over the South American Altiplano. *Mon Weather Rev* 128(9):3337–3346. [https://doi.org/10.1175/1520-0493\(2000\)128%3c3337:IVOMAR%3e2.0.CO;2](https://doi.org/10.1175/1520-0493(2000)128%3c3337:IVOMAR%3e2.0.CO;2)
- Garreaud RD (2009) The Andes climate and weather. *Adv Geosci* 22:3–11. <https://doi.org/10.5194/adgeo-22-3-2009>
- Garreaud RD, Aceituno P (2001) Interannual Rainfall Variability over the South American Altiplano. *J Clim* 14(1987):2779–2789. [https://doi.org/10.1175/1520-0442\(2001\)014%3c2779:IRVOT%3e2.0.CO;2](https://doi.org/10.1175/1520-0442(2001)014%3c2779:IRVOT%3e2.0.CO;2)
- Gill AE (1980) Some simple solutions for heat-induced tropical circulation. *Q J R Meteorol Soc* 106(449):447–462. <https://doi.org/10.1002/qj.49710644905>
- Gouirand I, Jury MR, Sing B (2012) An analysis of low- and high-frequency summer climate variability around the Caribbean antilles. *J Clim* 25(11):3942–3952. <https://doi.org/10.1175/JCLI-D-11-00269.1>
- Gu G, Adler RF (2018) Precipitation intensity changes in the tropics from observations and models. *J Clim* 31(12):4775–4790. <https://doi.org/10.1175/JCLI-D-17-0550.1>
- Houston J, Hartley AJ (2003) The central Andean west-slope rain-shadow and its potential contribution to the origin of hyper-aridity in the Atacama Desert. *Int J Climatol* 23(12):1453–1464. <https://doi.org/10.1002/joc.938>
- Hsu PC, Li T, Wang B (2011) Trends in global monsoon area and precipitation over the past 30 years. *Geophys Res Lett* 38(8):1–5. <https://doi.org/10.1029/2011GL046893>
- Hsu PC, Li T, Luo JJ, Murakami H, Kitoh A, Zhao M (2012) Increase of global monsoon area and precipitation under global warming: a robust signal? *Geophys Res Lett* 39(6):2–7. <https://doi.org/10.1029/2012GL051037>
- Hunziker S, Gubler S, Calle J, Moreno I, Andrade M, Velarde F, Ticona L, Carrasco G, Carrasco GY, Oria C, Croci-Maspoli M, Konzelmann T, Rohrer M, Brönnimann S (2017) Identifying, attributing, and overcoming common data quality issues of manned station observations. *Int J Climatol* 37(11):4131–4145. <https://doi.org/10.1002/joc.5037>
- Hurley JV, Vuille M, Hardy DR, Burns SJ, Thompson LG (2015) Cold air incursions, $\delta^{18}O$ variability, and monsoon dynamics associated with snow days at Quelccaya Ice Cap, Peru. *J Geophys Res Atmos* 120(15):7467–7487. <https://doi.org/10.1002/2015JD023323>
- Junquas C, Takahashi K, Condom T, Espinoza JC, Chavez S, Sicart JE, Lebel T (2018) Understanding the influence of orography on the precipitation diurnal cycle and the associated atmospheric processes in the central Andes. *Clim Dyn*. <https://doi.org/10.1007/s00382-017-3858-8>

- Kao A, Jiang X, Li L, Su H, Yung Y (2017) Precipitation, circulation, and cloud variability over the past two decades. *Earth Sp Sci* 4(9):597–606. <https://doi.org/10.1002/2017EA000319>
- Lagos P, Silva Y, Nickl E, Mosquera K (2008) El Niño related precipitation variability in Peru. *Adv Geosci* 3:231–237
- Lenters JD, Cook KH (1997) On the origin of the Bolivian high and related circulation features of the South American climate. *J Atmos Sci* 54(5):656–678. [https://doi.org/10.1175/1520-0469\(1997\)054%3c0656:OTOOTB%3e2.0.CO;2](https://doi.org/10.1175/1520-0469(1997)054%3c0656:OTOOTB%3e2.0.CO;2)
- Marengo JA, Tomasella J, Alves LM, Soares WR, Rodriguez DA (2011) The drought of 2010 in the context of historical droughts in the Amazon region. *Geophys Res Lett* 38(12):1–5. <https://doi.org/10.1029/2011GL047436>
- Martinez JA, Dominguez F (2014) Sources of atmospheric moisture for the La Plata River Basin. *J Clim* 27(17):6737–6753. <https://doi.org/10.1175/JCLI-D-14-00022.1>
- Melice JL, Roucou P (1998) Decadal time scale variability recorded in the Quelccaya summit ice core $\delta^{18}O$ isotopic ratio series and its relation with the sea surface temperature. *Clim Dyn* 14(2):117–132. <https://doi.org/10.1007/s003820050213>
- Minvielle M, Garreaud RD (2011) Projecting rainfall changes over the South American Altiplano. *J Clim* 24(17):4577–4583. <https://doi.org/10.1175/JCLI-D-11-00051.1>
- Morales MS, Christie DA, Villalba R, Argollo J, Pacajes J, Silva JS, Alvarez CA, Llancabure JC, Gamboa CC (2012) Precipitation changes in the South American Altiplano since 1300 AD reconstructed by tree-rings. *Clim Past* 8(2):653–666. <https://doi.org/10.5194/cp-8-653-2012>
- Neukom R, Rohrer M, Calanca P, Salzmann N, Huggel C, Acuña D, Christie DA, Morales MS (2015) Facing unprecedented drying of the Central Andes? Precipitation variability over the period AD 1000–2100. *Environ Res Lett* 10(8):84017. <https://doi.org/10.1088/1748-9326/10/8/084017>
- Nie J, Boos WR, Kuang Z (2010) Observational evaluation of a convective quasi-equilibrium view of monsoons. *J Clim* 23(16):4416–4428. <https://doi.org/10.1175/2010JCLI3505.1>
- Paccini L, Espinoza JC, Ronchail J, Segura H (2018) Intra-seasonal rainfall variability in the Amazon basin related to large-scale circulation patterns: a focus on western Amazon-Andes transition region. *Int J Climatol* 38(5):2386–2399. <https://doi.org/10.1002/joc.5341>
- Panthou G, Lebel T, Vischel T, Quantin G, Sane Y, Ba A, Ndiaye O, Diougue-Niang A, Diopkane M (2018) Rainfall intensification in tropical semi-arid regions: the Sahelian case. *Environ Res Lett* 13:6. <https://doi.org/10.1088/1748-9326/aac334>
- Perry LB, Seimon A, Kelly GM (2014) Precipitation delivery in the tropical high Andes of southern Peru: new findings and paleoclimatic implications. *Int J Climatol* 34(1):197–215. <https://doi.org/10.1002/joc.3679>
- Roberts J, Roberts TD (1978) Use of the Butterworth low-pass filter for oceanographic data. *J Geophys Res* 83(C11):5510–5514. <https://doi.org/10.1029/jc083ic11p05510>
- Rodwell MJ, Hoskins BJ (2001) Subtropical anticyclones and summer monsoons. *J Clim* 14(15):3192–3211. [https://doi.org/10.1175/1520-0442\(2001\)014%3c3192:SAASM%3e2.0.CO;2](https://doi.org/10.1175/1520-0442(2001)014%3c3192:SAASM%3e2.0.CO;2)
- Sakaguchi K, Leung LR, Burleyson CD, Xiao H, Wan H (2018) Role of troposphere-convection-land coupling in the Southwestern Amazon precipitation bias of the community earth system model version 1 (CESM1). *J Geophys Res Atmos* 123(16):8374–8399. <https://doi.org/10.1029/2018JD028999>
- Sassi F, Salby M, Read WG (2001) Relationship between upper tropospheric humidity and deep convection. *J Geophys Res* 106(D15):17133. <https://doi.org/10.1029/2001JD900121>
- Scala JR, Garstang M, Tao Wk, Pickering KE, Thompson AM, Simpson J, Kirchhoff VWJH, Browell EV, Sachse GW, Torres AL, Gregory GL, Rasmussen RA, Khalil MAK (2008) Cloud draft structure and trace gas transport. *J Geophys Res* 95(D10):17015. <https://doi.org/10.1029/jd095id10p17015>
- Schiro KA, Neelin JD, Adams DK, Lintner BR (2016) Deep convection and column water vapor over tropical land versus tropical ocean: a comparison between the Amazon and the Tropical Western Pacific. *J Atmos Sci* 73(10):4043–4063. <https://doi.org/10.1175/JAS-D-16-0119.1>
- Schneider T, Bordoni S (2008) Eddy-mediated regime transitions in the seasonal cycle of a Hadley circulation and implications for monsoon dynamics. *J Atmos Sci* 65(3):915–934. <https://doi.org/10.1175/2007JAS2415.1>
- Segura H, Espinoza JC, Junquas C, Takahashi K (2016) Evidencing decadal and interdecadal hydroclimatic variability over the Central Andes. *Environ Res Lett* 11(9):094016. <https://doi.org/10.1088/1748-9326/11/9/094016>
- Segura H, Junquas C, Carlo J, Vuille M, Jauregui YR, Rabatel A, Condom T, Lebel T (2019) New insights into the rainfall variability in the tropical Andes on seasonal and interannual time scales. *Clim Dyn*. <https://doi.org/10.1007/s00382-018-4590-8>
- Sherwood SC, Roca R, Weckwerth TM, Andronova NG (2010) Tropospheric water vapor, convection, and climate. *Rev Geophys* 48(2):1–29. <https://doi.org/10.1029/2009RG000301>
- Sicart JE, Espinoza JC, Quéno L, Medina M (2016) Radiative properties of clouds over a tropical Bolivian glacier: seasonal variations and relationship with regional atmospheric circulation. *Int J Climatol* 36(8):3116–3128. <https://doi.org/10.1002/joc.4540>
- Silva Dias PL, Schubert WH, DeMaria M (1983) Large-scale response of the tropical atmosphere to transient convection. *J Atmos Sci* 40(11):2689–2707. [https://doi.org/10.1175/1520-0469\(1983\)040%3c2689:LSROTT%3e2.0.CO;2](https://doi.org/10.1175/1520-0469(1983)040%3c2689:LSROTT%3e2.0.CO;2)
- Sulca J, Takahashi K, Espinoza JC, Vuille M, Lavado-Casimiro W (2018) Impacts of different ENSO flavors and tropical Pacific convection variability (ITCZ, SPCZ) on austral summer rainfall in South America, with a focus on Peru. *Int J Climatol* 38(1):420–435. <https://doi.org/10.1002/joc.5185>
- Vera C, Higgins W, Amador J, Ambrizzi T, Garreaud R, Gochis D, Gutzler D, Lettenmaier D, Marengo J, Mechoso CR, Noguez-Paele J, Dias PLS, Zhang C (2006) Toward a unified view of the American monsoon systems. *J Clim* 19(20):4977–5000. <https://doi.org/10.1175/JCLI3896.1>
- Vera CS, Diaz LB, Saurral RI (2019) Influence of anthropogenically forced global warming and natural climate variability in the rainfall changes observed over the South American Altiplano. *Front Environ Sci* 7(June):1–14. <https://doi.org/10.3389/fenvs.2019.00087>
- Virji H (1981) A Preliminary study of summertime tropospheric circulation patterns over South America estimated from cloud winds. *Mon Weather Rev* 109(3):599–610. [https://doi.org/10.1175/1520-0493\(1981\)109%3c0599:APSOST%3e2.0.CO;2](https://doi.org/10.1175/1520-0493(1981)109%3c0599:APSOST%3e2.0.CO;2)
- Vizy EK, Cook KH (2007) Relationship between Amazon and high Andes rainfall. *J Geophys Res Atmos* 112(7):1–14. <https://doi.org/10.1029/2006JD007980>
- Vuille M (2003a) Modeling $\delta^{18}O$ in precipitation over the tropical Americas: 1. Interannual variability and climatic controls. *J Geophys Res* 108(D6):4174. <https://doi.org/10.1029/2001jd002038>
- Vuille M (2003b) Modeling $\delta^{18}O$ in precipitation over the tropical Americas: 2. Simulation of the stable isotope signal in Andean ice cores. *J Geophys Res* 108:D6. <https://doi.org/10.1029/2001jd002039>
- Vuille M, Keimig F (2004) Interannual variability of summertime convective cloudiness and precipitation in the central Andes derived from ISCCP-B3 data. *J Clim* 17:3334–3348. [https://doi.org/10.1175/1520-0442\(2004\)017%3c3334:IVOSC%3e2.0.CO;2](https://doi.org/10.1175/1520-0442(2004)017%3c3334:IVOSC%3e2.0.CO;2)

- Vuille M, Hardy DR, Braun C, Keimig F, Bradley RS (1998) Atmospheric circulation anomalies associated with 1996/1997 summer precipitation events on Sajama Ice Cap, Bolivia. *J Geophys Res* 103(D10):11191. <https://doi.org/10.1029/98JD00681>
- Vuille M, Bradley RS, Keimig F (2000) Interannual climate variability in the Central Andes and its relation to tropical Pacific and Atlantic forcing. *J Geophys Res* 105(D10):12447. <https://doi.org/10.1029/2000JD900134>
- Vuille M, Kaser G, Juen I (2008) Glacier mass balance variability in the Cordillera Blanca, Peru and its relationship with climate and the large-scale circulation. *Glob Planet Change* 62(1–2):14–28. <https://doi.org/10.1016/j.gloplacha.2007.11.003>
- Wang XY, Li X, Zhu J, Tanajura CAS (2018) The strengthening of Amazonian precipitation during the wet season driven by tropical sea surface temperature forcing. *Environ Res Lett* 13(9):094015. <https://doi.org/10.1088/1748-9326/aadbb9>
- Wu CM, Stevens B, Arakawa A (2009) What controls the transition from shallow to deep convection? *J Atmos Sci* 66(6):1793–1806. <https://doi.org/10.1175/2008JAS2945.1>
- Zeng N, Yoon JH, Marengo Ja, Subramaniam A, Nobre Ca, Mariotti A, Neelin JD (2008) Causes and impacts of the 2005 Amazon drought. *Environ Res Lett* 3(1):014002. <https://doi.org/10.1088/1748-9326/3/1/014002>
- Zhang C, Chou MD (1999) Variability of water vapor, infrared radiative cooling, and atmospheric instability for deep convection in the equatorial western Pacific. *J Atmos Sci* 56(5):711–723. [https://doi.org/10.1175/1520-0469\(1999\)056%3c0711:VOWVIR%3e2.0.CO;2](https://doi.org/10.1175/1520-0469(1999)056%3c0711:VOWVIR%3e2.0.CO;2)
- Zhou J, Lau KM (1998) Does a monsoon climate exist over South America? *J Clim* 11(5):1020–1040. [https://doi.org/10.1175/1520-0442\(1998\)011%3c1020:DAMCEO%3e2.0.CO;2](https://doi.org/10.1175/1520-0442(1998)011%3c1020:DAMCEO%3e2.0.CO;2)
- Zhuang Y, Fu R, Marengo JA, Wang H (2017) Seasonal variation of shallow-to-deep convection transition and its link to the environmental conditions over the Central Amazon. *J Geophys Res Atmos* 122(5):2649–2666. <https://doi.org/10.1002/2016JD025993>

Publisher's Note Springer Nature remains neutral with regard to jurisdictional claims in published maps and institutional affiliations.